Role of the α4ß2 nicotinic acetylcholine receptor in stroke recovery

by

Angela Seto
B.Sc., University of Calgary, 2011

A Thesis Submitted in Partial Fulfillment
of the Requirements for the Degree of

MASTER OF SCIENCE

in the Department of Biology (Neuroscience)

Supervisory Committee

Role of the α4ß2 nicotinic acetylcholine receptor in stroke recovery

by

Angela Seto
B.Sc., University of Calgary, 2011

Supervisory Committee

Dr. Craig Brown (Division of Medical Sciences, Department of Biology)
Supervisor

Dr. Brian Christie (Division of Medical Sciences, Department of Biology)
Departmental Member

Dr. Raad Nashmi (Department of Biology)
Departmental Member

Abstract

Supervisory Committee
Dr. Craig Brown (Division of Medical Sciences, Department of Biology)
Supervisor
Dr. Brian Christie (Division of Medical Sciences, Department of Biology)
Departmental Member
Dr. Raad Nashmi (Department of Biology)
Departmental Member

Stroke is the leading cause of long-term disability in the developed world and can have devastating effects on the health and everyday functioning of individuals. In most cases stroke is ischemic and is caused by the obstruction of blood flow due to a clot in the brain blood vessels. This initiates a cascade of events that result in tissue death and loss of behavioural function associated with the damaged region. The peri-infarct cortex is a region surrounding the infarct core that survives the ischemic event and is most susceptible to pharmacological treatments and rehabilitation. α4ß2 nicotinic acetylcholine receptor (nAChR) signalling has been implicated as a mechanism that affects cell survival and cell death in the acute response after stroke. Nicotinic receptor signalling is also involved in modulating brain excitability, which can affect neural plasticity and restoration of cortical circuits and lead to recovery of lost function after stroke. In order to elucidate the role of α4ß2 nAChRs on acute and chronic recovery after stroke, we tested two hypotheses: (1) blocking α4ß2 nAChRs triggers acute neuroprotection and (2) α4ß2 nAChRs play a role in regulating plasticity and long-term functional recovery. In the first set of experiments a new model of targeted photothrombotic stroke was induced in a distal branch of the middle cerebral artery (MCA) in awake and anaesthetized mice. Mice treated with the α4ß2 nAChR antagonist dihydro-ß-erythroidine (DHßE) showed smaller lesion sizes relative to vehicle controls and this effect was greater in mice that were awake during stroke induction. To determine the mechanism of α4ß2 nAChR-mediated neuroprotection, changes in collateral flow were measured using Evans blue-stained surface angiograms and laser Doppler flowmetry. Contrary to what was expected, DHßE did not appear to induce neuroprotection by altering collateral flow. In the second set of experiments, we first used confocal imaging to quantify and characterize the expression of α4ß2 nAChRs after stroke. Next, mice were induced with a targeted

photothrombotic stroke in the forelimb somatosensory cortex. Mice were then chronically treated with DHßE to determine if α4ß2 nAChR antagonism could improve recovery of function. Behavioural tests showed that blocking α4ß2 nAChRs chronically had no effect on forelimb function after stroke. Voltage-sensitive dye imaging was used to measure forelimb-evoked responses in the somatosensory cortex and revealed no differences in cortical responsiveness between treated and non-treated groups. Altogether, these results show that changes in α4ß2 nAChR signalling that occur after stroke mediate ischemic cell death but do not have an effect on long-term recovery and plasticity. Moreover, they present a novel pathway for investigating stroke pathophysiology and the development of acute neuroprotective treatments.

Table of Contents

List of Tables

List of Figures

List of Abbreviations

AChE	Acetylcholinesterase
ACSF	Artificial cerebrospinal fluid
AMPA	α-Amino-3-hydroxy-5-methyl-4-isoxazolepropionic acid
ATP	Adenosine triphosphate
BBB	Blood brain barrier
BDNF	Brain-derived neurotrophic factor
CAMs	Cellular adhesion molecules
DHßE	Dihydro-β-erythroidine
DISC	Death-inducing signalling complex
FADD	Fas-associated death domain
FDA	U.S. Food and Drug Administration
FLS1	Forelimb primary somatosensory area
FLS2	Forelimb secondary somatosensory area
GABA	γ-Aminobutyric acid
GDNF	Glia-cell derived neurotrophic factor
GLT-1	Glutamate transporter-1
HLS1	Hindlimb primary somatosensory area
HLS2	Hindlimb secondary somatosensory area
LTP	Long-term potentiation
M1	Primary motor area
MAC	Mitochondrial apoptosis-induced channel
MCA	Middle cerebral artery
MMP	Matrix metalloproteases
MPT	Mitochondrial permeability transition pore
nAChR	Nicotinic acetylcholine receptor
NADH	Nicotinamide adenine dinucleotide
NF-κB	Nuclear factor-κB
NMDA	N-methyl-D-aspartate
nNOS	Neuronal nitric oxide synthase
NO	Nitric oxide
pCO_2	Carbon dioxide partial pressure
PIDs	Peri-infarct depolarizations
PAI-1	Plasminogen activator inhibitor type 1
pO_2	Oxygen partial pressure
ROS	Reactive oxygen species
(r)tPA	(Recombinant) tissue plasminogen activator
SD	Spreading depression
TGF-ß	Transforming growth factor-β
TNF-α	Tumor necrosis factor-α
TNFR	Tumor necrosis factor receptor
VEGF	Vascular endothelial growth factor

Acknowledgements

I would like to thank Dr. Craig Brown for his generous patience, mentorship, and the opportunity to do my thesis work in his lab. I also thank Drs. Raad Nashmi and Brian Christie for their insight and guidance throughout this project as members of my committee, and Dr. Paul Zehr for providing his time as the external examiner.

Without these individuals this work would not have been possible: Andrew Holmes, Dr. Kelly Tennant, Jessica Bilkey, Akram Zamani, Dustin Trudeau, Ryan Lim, Caitlyn Liu, Jay Leung, Patrick Reeson, Ian Swan, Karen Myers, Evelyn Wiebe, Danielle Sweetnam, Abdul Shehata, Dr. Josh Wang, fellow members of the Neuroscience graduate program, Mom, Dad, Allison, Adriana, Gordon, and Andrew. Thank you.

Chapter 1: Introduction

Stroke is a common brain disease that is ranked as one of the top three leading causes of death worldwide and the most significant cause of long-term adult disability (Lozano et al., 2012; Go et al., 2013). Major risk factors for stroke include hypertension, high cholesterol, obesity, diabetes, physical inactivity, age and race (Kissela et al., 2005; Boden-Albala et al., 2008; Go et al., 2013). For patients, the prognosis after stroke varies in terms of the type and severity of impairment, depending on where the stroke is located and the effectiveness and time-sensitivity of treatment, respectively. After a stroke 15-30% of patients face permanent disability with 20% placed in institutional care (Lloyd-Jones et al., 2010). There are approximately 300,000 survivors in Canada and 6.4 million in the United States living with the functional consequences of stroke (Lloyd-Jones et al., 2010; Public Health Agency of Canada, 2009). Stroke also imposes a financial burden on individuals and the economy. The average lifetime expense per person in the United States is estimated to be $140,048 for care after stroke, which adds to the physical, cognitive, and emotional strains that are placed on patients, their families, and their caretakers (Lloyd-Jones et al., 2010). Given the large population of individuals that do not recover fully and experience long-term effects of stroke in multiple facets of daily living, it is imperative for researchers to develop more effective treatment therapies that can enhance quality of life for affected individuals.

Since my thesis will examine how nicotinic receptors modulate both the acute and long-term effects of stroke, I will describe the cellular and molecular mechanisms of

ischemic cell death followed by those responsible for the repair of surviving brain circuits.

1.1 Acute Stroke and the Ischemic Cascade

A stroke is the disruption of blood flow to the brain, which results in cell death and subsequently a loss of brain function. There are two major categories of stroke: ischemic and hemorrhagic. In 87% of cases stroke is ischemic, which occurs when a clot reduces or occludes the blood supply to an area of the brain (Go et al., 2013). The clot originates in two ways: a thrombus is a clot that forms at the area of infarction in the artery, while an embolus travels from elsewhere in the body to the infarct region in the brain. The remaining 13% of cases are hemorrhagic and occur when weak blood vessels rupture and bleed into the surrounding tissue (Go et al., 2013). During a stroke the disrupted area is then deprived of energy and nutrients, and within four minutes following ischemic stroke structural damage starts to occur (Murphy et al., 2008). What follows the onset of stroke in the case of ischemia is a cascade of events that includes energetic failure, excitotoxicity, oxidative and nitrative stress, inflammation, peri-infarct depolarizations and apoptosis, all of which are complex and significant events that contribute to ischemic damage.

Energetic Failure and Osmotic Stress

Stroke initiates an ischemic cascade of events involving pathophysiological processes that occur over a matter of seconds, minutes, hours, and days (Fig. 1). These processes contribute either to immediate necrosis in the lesion core, or delayed apoptotic damage in the ischemic penumbra, the tissue surrounding the core that experiences hypoperfusion. The lesion core is where the damage is most severe and irreversible, while the penumbra

is still viable for a few hours after stroke onset due to reperfusion through collateral circulation (Hossmann, 1994). In the core, ischemia reduces oxygen and glucose levels and limits substrates available for oxidative phosphorylation including NADH (Welsh et al., 1982). This pathway almost exclusively generates the high levels of ATP required by the energy-demanding brain so that within 30 minutes of stroke onset, the ATP concentration is depleted and many ATP-dependent processes that participate in normal brain functioning break down (Welsh et al., 1982). In particular, ion pumps such as sodium/potassium (Na^+/K^+) ATPase and calcium (Ca^{2+}) ATPase cease to function. These pumps regulate ion gradients and membrane potential of the cell, so once they begin to fail, electrolyte concentration gradients become dysregulated such that extracellular K^+ increases while Na^+ and Ca^{2+} accumulates inside the cells (Hansen and Zeuthen, 1981; Harris et al., 1981; Siemkowicz and Hansen, 1981). The accumulation of sodium, calcium and bicarbonate inside cells promotes the passive movement of water inwards and ultimately cytotoxic edema (Beck et al., 2003). Cerebral edema, which includes cytotoxic and vasogenic edema, is a major factor in patient mortality following stroke, as it inhibits perfusion of the peri-infarct cells, increases intracranial pressure, and leads to compression of vasculature and brain herniation (Kunz et al., 2010).

Excitotoxicity

The breakdown of ion gradients and irreversible depolarization of neurons and glia in the infarct sets the stage for glutamate mediated excitotoxicity. Anoxic depolarization of cells leads to activation of voltage-gated Ca^{2+} channels, which regulate glutamate release and lead to a significant increase in the extracellular concentration of the excitatory amino acid (Benveniste et al., 1984; Murphy et al., 1988; Yaguchi and Nishizaki, 2010).

To further exacerbate the problem, sodium-dependent reuptake of the glutamate through the transporter subtype glutamate transporter-1 (GLT-1) is also disrupted, contributing to the accumulation of glutamate in the extracellular space (Ketheeswaranathan et al., 2011). The increase in intracellular sodium is coupled with the reversal of sodium-dependent glutamate transporters, which allows for the efflux of glutamate along its concentration gradient (Gemba et al., 1994). Excessive extracellular glutamate activates N-methyl-D-aspartate (NMDA) and α-amino-3-hydroxy-5-methyl-4-isoxazolepropionic acid (AMPA) receptors that flux Ca^{2+} into the cells (Gorter et al., 1997; Stanika et al., 2012). One outcome from the increase in intracellular calcium is the activation of proteases that degrade cytoskeletal proteins including actin and spectrin, compromising the integrity of the cell and vasculature (Hong et al., 1994; Hoang et al., 2010). In summary, normal electrical activity in the core only lasts for seconds to a few minutes into ischemia before ceasing altogether if reperfusion does not occur (Witte et al., 2000).

Oxidative and Nitrative Stress

One additional effect of increased calcium influx is the production of reactive oxygen species (ROS) and nitric oxide (NO). These free radicals are produced at high levels that outnumber endogenous antioxidants and react harmfully in the cell by creating membrane damage through lipid peroxidation and promoting apoptotic mechanisms (Adibhatla and Hatcher, 2003; Nanetti et al., 2011). The rise in intracellular calcium activates phospholipase A2, which releases arachidonic acid that in turn reacts in the cyclooxygenase pathway to form the superoxide anion ($\cdot O2^{-}$). During ischemia the Ca^{2+}/calmodulin-dependent neuronal nitric oxide synthase (nNOS) is also activated by the rapid influx of calcium and synthesizes nitric oxide (NO) from L-arginine at cytotoxic

levels. $\cdot O2^-$ and NO react together to produce peroxynitrite ($ONOO^-$), a highly unstable oxidant that can interact with DNA, proteins, and other cellular components to induce damage (Kristian and Siesjo, 1998). However, while NO generated through nNOS has detrimental effects, the endothelial NOS (eNOS) isoform produces NO in blood vessels that mediates vasodilation and activation of this pathway is associated with better outcome after stroke (Atochin et al., 2007). Free radicals are also produced from mitochondria during reperfusion and cause additional damage known as reperfusion injury. The ROS and calcium accrued in the cell during ischemia promotes swelling of mitochondria and formation of a mitochondrial permeability transition (MPT) pore (Friberg et al., 1998). This pore has high conductance that permits the indiscriminate flow of ions and molecules smaller than 1500 D. A consequence of MPT pore formation is the breakdown of the mitochondrial membrane potential, thereby preventing additional ATP production. This also leads to an additional surge in oxygen free radical production and eventually cell death (Piantadosi and Zhang, 1996; Kristian and Siesjo, 1998). Altogether, oxidative and nitrative stress induces detrimental processes that trigger structural damage in important cell structures and eventually widespread cell death.

Apoptosis

Apoptosis is a process that can last for days to even weeks after stroke onset, and occurs primarily outside the ischemic core. There are two activation pathways for caspase-dependent apoptosis signalling: an intrinsic and an extrinsic pathway. In the intrinsic pathway there are several cellular triggers that induce programmed cell death in the ischemic brain. DNA damage, free radicals, ionic imbalance, elevated intracellular calcium, mitochondrial swelling and mitochondrial apoptosis-induced channel (MAC)

formation in the outer mitochondrial membrane precipitate the release of cytochrome c (Sugawara et al., 2004; Broughton et al., 2009; Akpan and Troy, 2012). MAC is an early apoptotic marker that is regulated by the Bcl-2 gene family, which encodes pro-apoptotic (Bax and Bak) and anti-apoptotic (Bcl-2, Bcl-xL) proteins that induce or inhibit pore formation, respectively (Peixoto et al., 2011). The release of cytochrome c into the cytosol leads to formation of the apoptosome, a protein complex that includes cytochrome c bound to apoptotic peptidase activating factor 1 (Apaf-1), deoxyadenosine triphosphate (dATP), and procaspase 9. The apoptosome subsequently activates downstream caspases that are responsible for the systematic dismantling of cell structures (Broughton et al., 2009; Akpan and Troy, 2012). The extrinsic pathway is launched when ligands such as FasL bind cell surface death receptors from the tumor necrosis factor receptor (TNFR) family. FasL activates the Fas receptor (FasR) and enlists the Fas-associated death domain protein (FADD). FADD binds to procaspase 8 to produce the death-inducing signalling complex (DISC) (Sugawara et al., 2004; Akpan and Troy, 2012). This complex cleaves procaspase 8 and releases caspase 8 to activate a chain of caspases and initiate the cleavage of cell substrates. The aforementioned caspases 8 and 9 are categorized as cell death "initiator" caspases. There are three different types of caspases: apoptotic initiator (caspases 2, 8, 9, and 10), apoptotic effector (caspases 3, 6, and 7), or inflammatory (caspase 1 and 11). Initiator caspases cleave effector caspases into their active products while effector caspases go on to cleave other types of proteins to execute the cell death pathway throughout the cell (Akpan and Troy, 2012). Inflammatory caspases like caspase 1 cleave proinflammatory cytokines into their functional forms and increase the inflammatory response in the ischemic tissue. Within

the first twenty-four hours of ischemia, caspase gene expression is higher than normal. Caspase 3 is one of the major regulators of ischemia-induced apoptosis, as it is upregulated in the early stages of stroke in mouse and human tissue (Namura et al., 1998; Rami et al., 2003). Studies have demonstrated that inhibition of caspase 3 activity is correlated with decreased injury, which indicates that targeting these enzymes to block progression of the apoptotic pathway is a potential avenue for treatment after stroke (Fink et al., 1998; Le et al., 2002).

Inflammation

Normally the body's immune response operates beneficially, as its function is to clear away foreign and harmful antigens that threaten the health of tissue. During ischemia, however, the immune system can promote a chronic inflammatory response using pathways that antagonize cell damage and the viability of the ischemic penumbra. The neuroinflammatory response incorporates a variety of players from the cellular to the protein level that either encourage or prevent peri-infarct cells from being recruited into the lesion core (Graham, 2011). During the neuroinflammatory response ischemia typically stimulates glia that surround the injured neurons. This includes microglia and astrocytes, cells that ordinarily work to support neuronal health. Once microglia and astrocytes are activated, they begin to release pro- and anti-inflammatory molecules that can compromise blood brain barrier (BBB) integrity, promote edema, degrade proteins, phagocytose debris, and promote angiogenesis and plasticity (Lakhan et al., 2009; Graham, 2011; Iadecola and Anrather, 2011). These inflammatory mediators include cytokines, chemokines, and matrix metalloproteases (MMPs) that interact with adhesion molecules and leukocytes that modulate ischemic death.

Cytokines are glycoproteins that are usually expressed at very low concentrations but are massively accumulated during ischemia (Sieber et al., 2013). Pro-inflammatory cytokines include interleukin-1ß (IL-1ß), IL-6, and tumor necrosis factor-α (TNF-α). These cytokines worsen stroke outcome by stimulating the production of pro-inflammatory cytokines and adhesion molecules, and inhibiting the reuptake of glutamate into cells (Ye and Sontheimer, 1996; Lakhan et al., 2009). They also stimulate activation of more astrocytes and glia, compounding the inflammatory response even further. Meanwhile, anti-inflammatory cytokines are neuroprotective and serve to ameliorate the neuronal loss. Transforming growth factor-ß (TGF-ß) and IL-10 are the two major anti-inflammatory proteins involved in reducing stroke damage. These cytokines reduce the activation of glial cells and inhibit IL-1ß and TNF-α as well as their receptor expression (Lakhan et al., 2009; Graham, 2011). Chemokines are a family of cytokine that are involved in migrating inflammatory cells from the blood vessels into the injured tissue. They are also normally expressed in the brain at low levels and are quickly upregulated after stroke (Sieber et al., 2013). Chemokines function by attracting leukocytes such as neutrophils and monocytes down a concentration gradient towards the ischemic region. Thirdly, matrix metalloproteases are enzymes that degrade elements of the extracellular matrix, and in stroke they facilitate breakdown of the BBB by targeting basal lamina proteins (Lakhan et al., 2009; Kunz et al., 2010). MMP-2 and MMP-9 are implicated in ischemic injury and are supplied by endothelial cells, neutrophils and macrophages. Studies applying early inhibition of MMP activity have shown reduced apoptotic cell death and infarct volume following middle cerebral artery occlusion (Romanic et al., 1998; Lakhan et al., 2009; Hill et al., 2012).

Following ischemia, increased permeability of the BBB permits movement of molecules through the endothelium. Adhesion molecules facilitate diapedesis of leukocytes through the BBB that stands between blood vessels and brain parenchyma. These molecules are separated into three groups: selectins, integrins, and immunoglobulin superfamily cellular adhesion molecules (CAMs) (Graham, 2011). Carbohydrate ligands on the surface of neutrophils and monocytes are bound by selectins to slow down the traveling cells and facilitate leukocytes rolling over the endothelium walls. Selectin production implicated in stroke occurs from endothelial cells (E-selectins) and platelets (P-selectins) and is stimulated by cytokines and other pro-inflammatory molecules. Integrins are expressed by neutrophils and monocytes and attach to receptors on the endothelium to tightly bind and prevent movement along the endothelial wall. This secure attachment is supported by CAMs, which subsequently help pull the leukocytes through the BBB (Lakhan et al., 2009; Graham, 2011). Suppression of adhesion molecule expression is correlated with lower levels of neutrophil migration and less tissue damage, which suggests that these molecules mediate ischemic injury during the inflammatory response (Hu et al., 2004). In the microvasculature, with the help of adhesion molecules, neutrophils build up on the endothelial walls and obstruct the vessels, prohibiting reperfusion in what is called the “no-reflow” phenomenon. Preventing the adherence of leukocytes to endothelium walls allows for greater recovery of blood flow (Mori et al., 1992).

Although many substances released tend to be harmful to the evolving ischemic tissue as described above, there are some virtues of the chronic inflammatory response. Microglia and astrocytes also produce beneficial growth factors such as brain-derived

neurotrophic factor (BDNF), glia cell-derived neurotrophic factor (GDNF), and vascular endothelial growth factor (VEGF) to support cell survival (Iadecola and Anrather, 2011). When cells become ischemic, microglia relocate towards the lesion site and "cap" injured neurons so that once they die, they are quickly detected and removed (Neumann et al., 2006). Furthermore, astrocytes quickly form glial scar tissue after injury to prevent the spread of infections and cell damage (Carmichael et al., 2005). Overall, it may be possible that the early phase of the glial activation that mediates inflammation is harmful to the brain, while during later stages of ischemia, the immune system yields more beneficial effects.

Peri-infarct Depolarizations (PIDs)

While anoxic depolarizations occur in the ischemic core, the peri-infarct tissue experiences massive waves of repetitive depolarizations that are a result of excessive glutamate and potassium release and can last for hours (Nedergaard and Astrup, 1986; Busch et al., 1996). These depolarizations propagate onwards to normal tissue as waves of spreading depression (SD). SD in healthy tissue does not cause damage, as cell membranes can quickly repolarize and re-establish ion gradients. However, depolarizations in the peri-infarct region add exceptional stress to already-compromised tissue and can cause regions of the penumbra to join the lesion core (Hossmann, 1994). Studies have shown that PIDs induce structural damage, such as dendritic beading and spine loss, that is reversible only with adequate blood flow (Risher et al., 2010). The frequency of PIDs correlates positively with infarct core growth and can be attenuated by NMDA receptor antagonists such as MK-801 (Busch et al., 1996). In summary, electrical events that are well tolerated in the healthy brain parenchyma cause devastating effects in

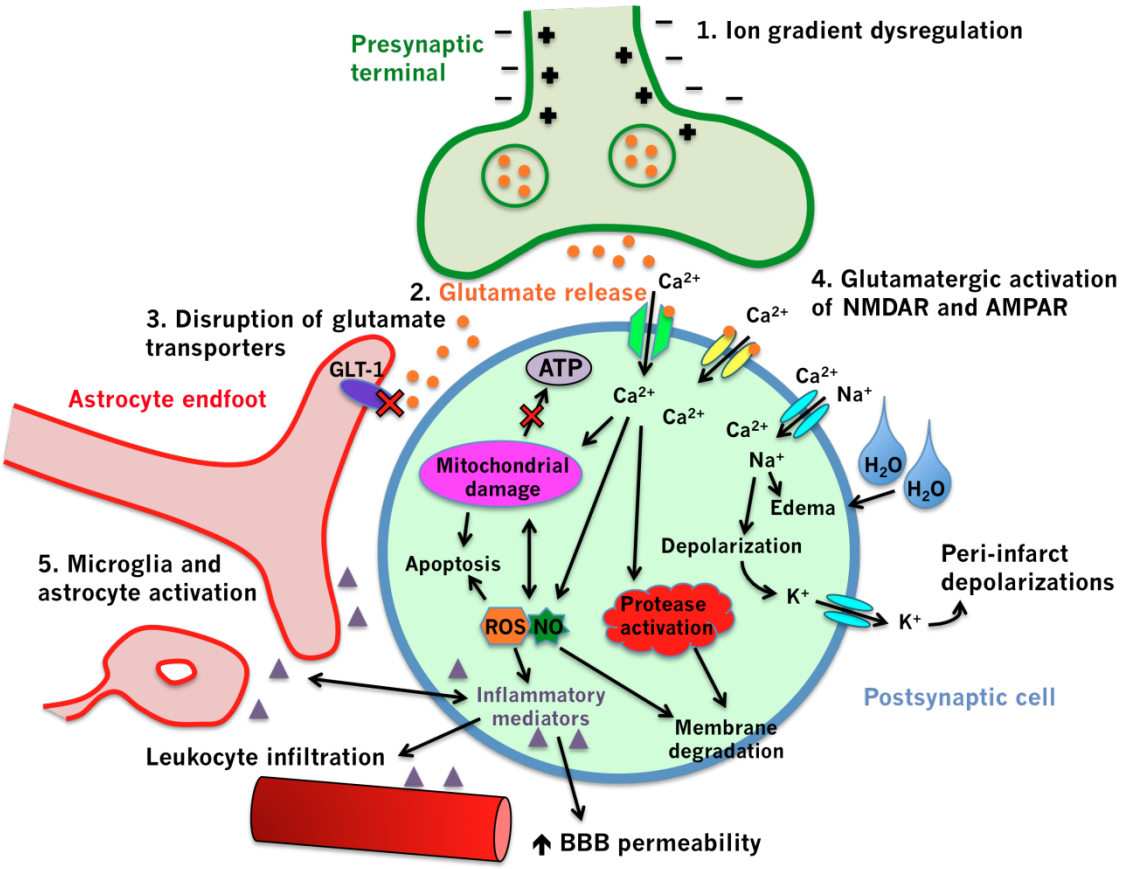

Figure 1. Cascade of ischemic processes that occur during stroke.

This figure was adapted from Dirnagl et al. (1999). **1.** Energetic failure in the cell leads to breakdown of ATP-dependent processes and dysregulation of ion gradients. Consequently there is an increase in extracellular K^+ and an accumulation of intracellular Ca^{2+} and Na^+. The increase in intracellular cations promotes cytotoxic edema and anoxic depolarizations, which go on to propagate through penumbral tissue as peri-infarct depolarizations. **2.** Anoxic depolarization leads to release of glutamate into the extracellular space. **3.** The accumulation of extracellular glutamate is further exacerbated by the disruption and reversal of glutamate reuptake mechanisms. **4.** High levels of extracellular glutamate activate NMDA (green) and AMPA (yellow) receptors, which flux even more Ca^{2+} into the cell. Intracellular Ca^{2+} activates processes such as reactive oxygen species (ROS) and nitric oxide (NO) production, mitochondrial damage, and protease activation. These mechanisms go on to induce cell damage through membrane degradation, DNA damage, apoptosis, and preventing additional ATP production. **5.** The release of inflammatory mediators by ROS activates microglia and astrocytes, which release even more inflammatory molecules that promote infiltration of leukocytes into blood vessels, increases BBB permeability, and triggers further apoptosis.

the vulnerable penumbra due to the altered chemical environment as a result of stroke.

1.2 Plasticity and Long-term Recovery from Stroke

Once cells have survived past the acute period of ischemic cell death (first 24 hours), the main goal for researchers and clinicians is to promote recovery of functions associated with damaged brain areas. The peri-infarct cortex is a region surrounding the infarct core that survives the ischemic event, but has abnormal metabolism, perfusion and electrical activity, especially during the first week of stroke recovery. This area of brain tissue is most susceptible to pharmacological interventions and rehabilitation, and can be targeted to restore lost function from the damaged regions (Murphy and Corbett, 2009). Recovery from stroke is typically defined as the progressive reduction in sensory, motor and cognitive disturbances following injury. Most of the time it is difficult to obtain "true" and full recovery, where the ability to sense or move the body returns to pre-stroke levels (i.e. "good as new"), due to the loss of neurons that are highly specialized to certain tasks. However, it is known that the brain can repair and re-establish damaged pathways to allow for at least partial restoration of sensory/motor function, as well as modify behavioural strategies to achieve a goal (Murphy and Corbett, 2009).

Although ischemic stroke activates a cascade of detrimental processes, it also induces an environment that promotes a high level of plasticity in peri-infarct tissue. Structural and functional changes are observed extensively in the peri-infarct cortex, which lead to improvements in behaviour. In the brain, there is a large amount of dispersed and redundant connections that can compensate, to a certain extent, for disruptions in signal transmission. Using these distributed connections gives the brain the ability to restore

impaired function after a stroke. In the initial days after a stroke, stimulation of the impaired limb is associated with heightened activation of the contralesional cortex and depressed responses in the peri-infarct cortex (Dijkhuizen et al., 2001, 2003). After several weeks of recovery, the peri-infarct region begins to respond strongly to stimulation again as new connections are formed within this area (Dijkhuizen et al., 2001, 2003; Brown et al., 2009; Sweetnam et al., 2012). Typically, the more remapping of function that occurs in the peri-infarct hemisphere, the better the behavioural outcome is for patients, whereas sustained bilateral activation after several weeks is correlated with worse outcome (Dijkhuizen et al., 2003). This evidence suggests that bilateral activation only persists when the brain is unable to re-establish normal, lateralized activation of the peri-infarct cortex through remapping and compensatory mechanisms.

Research has shown that remapping of brain function also involves the formation of new circuits that are distal but functionally related to the lesion area. After stroke there is increased turnover of dendritic spines that persists for up to six weeks, and the high turnover coincided with a return to control spine density levels (Brown et al., 2007, 2009). Within two weeks of recovery, significant transformation of dendritic arbors is observed in the form of dendritic tip growth and retraction (Brown et al., 2010). Before stroke, dendritic tufts appear weaved together without any distinct patterning, whereas peri-infarct dendritic tufts are revealed to extend from the border of the infarct (Brown et al., 2007). Given the dynamic nature of dendritic structure, and taking into consideration their role as the main target for excitatory synapses in the CNS, it is plausible that changes in dendritic spines and arbors are important mechanisms of stroke recovery.

Axonal plasticity is another candidate underlying the restoration and development of functional circuits related to the infarct area. In squirrel monkeys, loss of input to the ventral premotor cortex (PMv) following stroke in the hand motor cortex resulted in the proliferation of new axonal projections from the PMv to the primary somatosensory region (Dancause et al., 2005). Furthermore, after eight weeks of recovery from stroke in the forelimb somatosensory region in mice, functional connections from the retrosplenial cortex and the ipsilateral striatum to the peri-infarct cortex were revealed using tract tracing and voltage sensitive dye (VSD) imaging (Brown et al., 2009). These new connections, along with remodeling in the peri-infarct cortex, are reflective of axonal sprouting and morphological changes in dendritic structure. One obstacle to sprouting in the normal adult brain is the inhibitory environment. Typically this inhibition is mediated by growth-inhibitory myelin-associated proteins, extracellular matrix proteins, and developmentally associated growth cone inhibitors (Carmichael 2006). Stroke induces an environment of altered gene and protein expression that permits axonal sprouting in the peri-infarct cortex (Carmichael et al., 2001; Dancause et al., 2005). The glial scar formed by astrocytes as an inflammatory response contains elevated levels of growth-promoting and growth-inhibitory factors (Carmichael et al., 2005). Adjacent to the glial scar is an area of the peri-infarct tissue where the growth-inhibitory factors are reduced and growth-promoting proteins are increased, creating a growth-permissive zone where axonal sprouting is stimulated. Growth promoting factors such as growth-associated protein 43 (GAP43) and cytoskeleton-associated protein 23 (CAP23), along with the transcription factor c-JUN show increased and sustained mRNA expression for at least twenty-eight days after stroke (Carmichael et al., 2005). This upregulation is limited to areas that

undergo axonal sprouting and their expression declines further away from the infarct area in a graded manner. With increased axonal sprouting it is important to know whether or not there is also an associated increase in synaptic connections that can underlie the remodeling of cortical circuits in the peri-infarct cortex. Stroemer et al. (1995) showed that GAP43 expression peaks in peri-infarct regions in the first 2 weeks of stroke recovery that was followed by a protracted period of synapse formation that lasted up to 60 days post-stroke. These changes were positively associated with behavioural performance and imply that promoting axonal sprouting and synaptogenesis is indeed linked to rewiring processes required for enhanced recovery after stroke.

Another mechanism that is potentially responsible for fostering neural plasticity after stroke involves alterations in neuronal circuit excitability. At the present time, there is considerable debate as to whether stroke promotes excitation or inhibition. For instance, work from Otto Witte's group has demonstrated in a series of electrophysiological experiments that pyramidal cells in the peri-infarct show reduced paired-pulse inhibition, a depolarizing shift in mean resting membrane potential, and increased long-term potentiation (LTP) compared to controls (Domann et al., 1993; Neumann-Haefelin et al., 1995; Hagemann et al., 1998). This evidence is complimented by autoradiography and immunohistochemistry labelling studies that reveal significant lowering of γ-aminobutyric acid (GABA) receptor subunit A levels in the peri-infarct cortex (Schiene et al., 1996; Redecker et al., 2002). Collectively, these studies suggest that stroke can enhance peri-infarct excitability either directly or through dis-inhibition of inhibitory networks which can support the strengthening of connections in an activity-dependent manner.

Stroke can also enhance tonic inhibition, an inhibitory phenomenon that requires the binding of ambient levels of GABA to $GABA_A$ receptors located on peri- or extra-synaptic sites (Farrant and Nusser, 2005). The resulting current is much more long-lasting compared to phasic (or synaptic) GABA receptor mediated activation and governs the overall membrane potential and propensity for the cell to fire. When the brain undergoes ischemia, the level of tonic inhibition in the peri-infarct is immediately heightened and lasts for over six weeks (Clarkson et al., 2010). In the acute stage this may be a neuroprotective response to the excitotoxic events that occur immediately following stroke, however in the long run this effect is counterproductive towards plasticity. Indeed, administration of a $GABA_A$ receptor antagonist reduced tonic inhibition and when given three days after stroke, motor function in mice was enhanced as early as one week after stroke (Clarkson et al., 2010). Furthermore, studies that increase excitability in the brain after stroke by enhancing glutamatergic signalling through AMPA receptors can improve behavioural outcome. Although stimulating AMPA receptors immediately after stroke exacerbates cell death and infarct damage, chronic administration of an AMPA receptor agonist after five days improved behavioural recovery significantly by four weeks after stroke, and blocking this system not only negated this effect but also worsened normal recovery in an animal model (Clarkson et al., 2011). It is apparent then that stroke triggers changes in excitability that fluctuate over time and influence processes mediating recovery and functional outcome.

1.3 Cholinergic Signalling and Stroke

Acetylcholine was first discovered by Sir Henry Dale in 1914 and described in the peripheral nervous system as a potent agonist for the parasympathetic response (Tansey,

2006). It is now known that the cholinergic system projects throughout the brain and modulates a myriad of pathways involved in reward, attention, cognition, learning and memory, mood, and sensory processing (Granon et al., 1995; Paterson and Nordberg, 2000; Terry et al., 2000; Metherate, 2004; Miwa et al., 2011). Dysfunction of cholinergic signalling is also implicated in disease states such as Alzheimer's, Parkinson's, and myasthenia gravis (Pimlott et al., 2004; Buckingham et al., 2009; Miwa et al., 2011). Acetylcholine exerts its effects on two different receptor subtypes. Muscarinic acetylcholine receptors are metabotropic G-protein complexes that bind to muscarine along with endogenous acetylcholine (Brown, 2010). Nicotinic acetylcholine receptors are ionotropic channels that have binding specificity to nicotine (Nashmi et al., 2007). The role that acetylcholine transmission plays in stroke pathophysiology has been relatively unexplored compared to other neurotransmitters, but there is some evidence that suggests that nicotinic acetylcholine receptor activation might be involved (Hawkins et al., 2002; Furukawa et al., 2012). However, its role in chronic stroke recovery has been inconclusive, and remains to be investigated as a potential target for therapeutic treatment.

Nicotinic Receptors

Nicotinic acetylcholine receptors (nAChRs) are ligand-gated ion channels that flux sodium, potassium, and calcium ions and are largely found in the nervous system and the neuromuscular junction, on both neural and glial cells (Galzi and Changeux, 1995; Millar and Gotti, 2009; Zouridakis et al., 2009). They are part of the Cys-loop family of receptors that also include 5-HT_3, $GABA_A$, and glycine receptors (Nashmi and Lester, 2006; Millar and Gotti, 2009; Zouridakis et al., 2009). The structure of the nAChR was

first described in 1993 by Nigel Unwin, who developed a model of the receptor from the *Torpedo* electric ray using electron microscopy. The receptors consist of five subunits that make up a barrel-like formation surrounding a central pore (Unwin, 1993, 1998, 2005). Currently 17 vertebrate subunits have been identified that fall into five types: α subunit (α, α2-α10), ß-subunit (ß, ß2-ß4), γ, ∂, and ε (Millar and Gotti, 2009; Zouridakis et al., 2009). These subunits assemble in various combinations to form distinct receptor subtypes with unique pharmacological and signalling properties. Nicotinic receptors subtypes are categorized as 'muscle-type,' or 'neuronal' based on their expression in muscle cells or the nervous system respectively. In the periphery, muscle-type nAChRs contain α, ß, ∂, and γ/ε (γ in embryonic muscle, ε in adult) subunits (Millar and Gotti, 2009; Zouridakis et al., 2009). In neuronal nAChRs there are only two different subunits that make up the pentamer, α and ß (Whiting and Lindstrom, 1986a; Sargent, 1993; Millar and Gotti, 2009; Zouridakis et al., 2009). These include α2-α10 and ß2-ß4 and are typically arranged in heteromeric combinations, with the exception of certain receptors types containing only one form of subunit (α7 or α8 only) in a homomeric pentamer (Anand et al., 1991; Millar and Gotti, 2009). The most common subtypes of nicotinic receptors in the central nervous system are the heteromeric α4ß2 nAChRs, which desensitize slowly and have high affinity for nicotine (in the 0.1-1 μM range), and homomeric α7 nAChRs that have lower affinity for nicotine (EC_{50} = 90 μM) and acetylcholine and desensitize rapidly (Whiting and Lindstrom, 1986b; Zhang et al., 1994; Fenster et al., 1997; Alkondon et al., 2000). α7 nAChRs are also notable for their high calcium conductance similar to that of NMDA receptors (Séguéla et al., 1993). At the subcellular level, nAChRs are located on the soma, dendrites, and axon terminals,

implicating their involvement in both pre- and post-synaptic signalling (Alkondon et al., 1996; Jones et al., 2001; Jones and Wonnacott, 2004; Nashmi et al., 2007; Brown et al., 2012).

The α4ß2 receptor is the most prevalent neuronal nicotinic receptor that was first described by Whiting and Lindstrom (1986), who purified the receptor from the chick brain. Distribution of α4ß2 nAChRs is widespread throughout the brain, particularly in regions such as the thalamic and interpeduncular nuclei (Wada et al., 1989; Nashmi et al., 2007). The α4ß2 receptor can be further separated into two major isoforms based on stoichiometry. $(\alpha4)_2(ß2)_3$ receptors show extremely high sensitivity to acetylcholine and nicotine, are thought to be expressed mainly on presynaptic terminals, and can be activated at concentrations of 0.1 to 1 μM of either agonist (Nelson et al., 2003). Meanwhile, $(\alpha4)_3(ß2)_2$ receptors have lower affinity towards nicotine but exhibit greater permeability to Ca^{2+} (Nelson et al., 2003; Tapia et al., 2007). The role of nicotinic receptors in the brain is not precisely defined, but they are thought to have a role in altering neuron excitability by modulating pre-synaptic release of other types of neurotransmitters such as dopamine, noradrenaline, serotonin, GABA, and glutamate or by depolarizing post-synaptic membranes (Wonnacott, 1997; Kenny et al., 2000; Lambe et al., 2003; Xiao et al., 2009b; Nakamura and Jang, 2010). Nicotine likely enhances pre-synaptic GABA release as evidenced by nicotine evoked increases in the frequency of spontaneous inhibitory postsynaptic currents (sIPSCs) that are blocked by the α4ß2 nAChR antagonist DHßE (Xiao et al., 2009a, 2009b). Nicotine has also been shown to increase the frequency of spontaneous excitatory postsynaptic currents (sEPSCs), an effect that is blocked with DHßE application and absent in ß2 nAChR subunit knockout

mice, indicating that nicotine also facilitates pre-synaptic release of glutamate (Lambe et al., 2003). Additionally, in experiments looking at experience-dependent plasticity, mice that underwent whisker trimming showed a decrease in peak cortical responses to whisker stimulation that corresponded with an upregulation of α4ß2 receptors on GABAergic neurons in the barrel cortex. Furthermore, the depression of sensory-evoked cortical responses could be mimicked by applying an α4ß2 receptor agonist to the brain or inhibited by chronically treating mice with an α4ß2 receptor antagonist DHßE (Brown et al., 2012). Together, these studies demonstrate that cholinergic α4ß2 receptor signalling can regulate neuronal excitability in a cell-specific manner.

The α4ß2 Nicotinic Receptor and Stroke

The notable role that α4ß2 receptors play in modulating excitability within neural circuits has potential implications in the pathophysiology of ischemic stroke. However, limited research exists that has fully explored this possibility. Cell culture studies have also shown that pre-treatment with nicotine prevents intracellular calcium increases and supports cell survival following glutamate-mediated neurotoxicity by inactivating L-type Ca^{2+} channels, and this effect is regulated by ß2-subunit containing nAChRs in cooperation with α7-receptors (Stevens et al., 2003). However, simultaneous nicotine treatment with glutamate toxicity did not produce any beneficial effects, so the role that these receptors play when activated *after* injury is unclear (Akaike et al., 1994; Stevens et al., 2003). Finally, while α7 receptors have been widely implicated in the inflammatory process, there is some research in peripheral systems that point to α4ß2 receptor involvement as well. During the inflammatory response, activation of α4ß2 nicotinic receptors in cell culture suppresses constitutive NF-κB pathway activity, which leads to

reduced production of the pro-inflammatory cytokines IL-1ß and IL-6 in neuroblastoma cells (Hosur and Loring, 2011). From these studies it is apparent that α4ß2 nicotinic receptors may be involved in processes that are part of the ischemic cascade or long-term recovery. How these receptors interact specifically in stroke pathology is currently not well understood and remains to be explored.

1.4 Photothrombotic Model of Ischemic Stroke

Photothrombosis was developed by Watson et al. (1985) as a targeted and reproducible method of inducing ischemic stroke in the cortex. This method photochemically produces singlet oxygen species and platelet aggregation in the targeted blood vessels using a photosensitizing organic dye that is activated by an excitatory light wavelength. Singlet oxygen is a highly reactive molecule that causes damage to endothelial cells on the lumen surface through lipid peroxidation, and this elicits a high volume of platelet aggregation that leads to formation of a thrombus at the site of activation (Herrmann, 1983). Dyes that are used for photoactivation include fluorescein isothiocyanate, rose bengal, and erythrosine B. Rose bengal is most commonly used because of its high efficacy generating singlet oxygen and ability to cause infarction of larger volumes of brain relative to other photosensitizing agents (Watson et al., 1985). Advantages of this method include reproducibility, minimal invasiveness and no mechanical interference with brain tissue or vessels. Furthermore, rose bengal is activated when exposed to 532-560 nm light and thrombogenesis is restricted to only vessels that are irradiated by this wavelength (Watson et al., 1985; Sweetnam et al., 2012). Therefore, photothrombosis can be targeted in terms of lesion size, severity, and location. However, there are some limitations to this method. The ischemic penumbra produced is very small compared to other models and

the region of reperfusion is limited. Moreover, there is a significant local vasogenic edema response along with cytotoxic edema that happens early on after photothrombosis that is unlike what occurs in human stroke, which is cytotoxic edema alone as an acute response (Carmichael, 2005). Nevertheless, its ability to induce focal lesions reproducibly has allowed this model of stroke to be very useful for exploring changes in neurotransmission, cortical excitability, and cell structure after stroke in both peri-infarct and contralateral cortex (Carmichael, 2005).

1.5 Rationale

Although nAChRs play an important role in modulating brain excitability and plasticity, very little is known about how they regulate stroke damage or recovery. In the first set of experiments, we examined how α4ß2 nAChRs affect ischemic cell death and collateral blood flow using a new model of distal middle cerebral artery occlusion. In the second set of experiments, we tested the hypothesis that α4ß2 nAChRs play an important role in regulating the plasticity/rewiring of cortical circuits and recovery of function after stroke.

Chapter 2: Acute Neuroprotection Following Ischemic Stroke

2.1 Introduction

Within seconds of stroke onset, cell death begins in the ischemic core as tissue is deprived of valuable nutrients that are delivered via the cerebrovascular system. This follows the initiation of the ischemic cascade: a variety of events including energy failure within cells, excitotoxicity, overproduction of free radicals leading to oxidative stress, dysfunction of the blood-brain barrier, and post-ischemic inflammation (Welsh et al., 1982; Murphy et al., 1988; Lakhan et al., 2009; Nanetti et al., 2011). These events can last in the ischemic penumbra for hours, which means that neuroprotective strategies that target these processes can be implemented soon after stroke to salvage vulnerable cells that surround the ischemic core. One way to save the penumbra is by restoring blood flow to the occluded areas. For patients and clinicians, it is important to restore blood flow as soon as possible after stroke onset as time to reperfusion is highly correlated with improved stroke outcome (Nogueira et al., 2011). The only FDA-approved treatment therapy for ischemic stroke currently available is recombinant tissue plasminogen activator (rtPA), which lyses the thrombus to allow blood flow to return to the obstructed vessel. However, rtPA also has a risk of causing hemorrhage after a certain period of ischemia and therefore can only be used in a small subset of patients that qualify for treatment (NINDS, 1995). Another means by which the ischemic tissue undergoes reperfusion is through collateral circulation from supplementary vasculature near the ischemic region. Adjacent vessels anastomose to the distal branches of the obstructed vessel during and after a stroke to provide a limited degree of collateral blood flow

(Liebeskind, 2003; Armitage et al., 2010). It has been shown that middle cerebral artery occlusion induces anastomosis between the anterior and middle cerebral arteries (Armitage et al., 2010). Infarct volume is correlated with the degree of collateral flow, and patients with poor collateral circulation tend to show greater lesions relative to patients with better collateral circulation (Bang et al., 2009).

Nicotinic receptor activity during stroke has not been well characterized and its effects on acute neuroprotection are still unclear. Activation of α4ß2 nAChRs has been shown to transiently elevate cerebral blood flow in healthy mice, but this effect is ameliorated by chronic high-dose nicotine pre-treatment (Uchida et al., 1997, 2009). Pre-treatment with nicotine in cell culture also protects neurons from glutamate excitotoxicity but this response is not observed when receptor activation occurs concurrently with excitotoxicity (Stevens et al., 2003). Meanwhile, agonism of α4ß2 nAChRs by nicotine appears to induce the release of glutamate in the prefrontal cortex, a response that can contribute to increased excitotoxicity in ischemic conditions (Lambe et al., 2003). Nicotine and cytisine application has also been shown to induce spreading depression, which is extremely stressful for vulnerable cells in the penumbra and can subsequently result in greater tissue damage (Sheardown, 1997). Additionally, perinatal exposure to nicotine exacerbates tissue injury in hypoxic-ischemia studies, suggesting that neurons become more vulnerable to ischemic damage with increased nAChR activation during gestation (Li et al., 2012). These data suggest that nicotinic receptor activation during stroke might result in a poorer outcome. It is therefore possible that blocking nicotinic receptor during stroke could have neuroprotective effects.

In this study we investigated the role of α4ß2 nAChRs in ischemic stroke using a novel protocol that eliminates the use of general anaesthesia for stroke induction. Virtually all existing experimental models of ischemic stroke require the use of general anaesthetics such as isoflurane. This poses a problem because anaesthetics also interfere with neurotransmitter signalling, blood flow, and cell death pathways, which can confound the effects induced by a stroke treatment (Schwinn et al., 1990; Moody et al., 1993; Dickinson et al., 2007; Zhang et al., 2012). Isoflurane has been to shown to be neuroprotective when administered before, during, and even after stroke (Kapinya et al., 2002; Khatibi et al., 2011; Bleilevens et al., 2012). Binding sites for isoflurane have been found on the *Torpedo* nAChR transmembrane domain, and isoflurane appears to potently inhibit α4β2 nAChRs (Flood et al., 1997; Rada et al., 2003; Brannigan et al., 2010). Given that isoflurane influences the action of α4β2 nAChRs as well as several processes characteristic of stroke pathophysiology, it is important to assess the efficacy of our stroke therapy without the interference of isoflurane.

Objective and Hypothesis

The objective of this study was to determine the role of α4ß2 nAChRs in acute neuroprotection. We hypothesized that suppressing α4β2 nAChR signalling elicits a neuroprotective response and reduces ischemic damage. We tested this hypothesis by inducing an ischemic stroke in the distal branch of the middle cerebral artery (MCA) in freely moving and anaesthetized mice. Animals received treatment of α4ß2 nAChR specific antagonist dihydro-β-erythroidine (DHβE) or vehicle and infarct volumes were assessed at two acute stages after stroke. We measured the extent of reperfusion through collateral circulation in the distal MCA at each time point using confocal imaging. To

measure changes in blood perfusion in the cortical penumbra, we used laser Doppler flowmetry. Heart and respiration rate, blood gas, pH, and electrolyte content were also analyzed to detect any physiological changes between groups.

2.2 Methods

Animals

Ninety adult (2-4 months old) male wild-type or YFP-H line mice with C57BL/6J background were used (Feng et al., 2000). All experiments were conducted in accordance with guidelines set by the Canadian Council for Animal Care. Mice were group housed under a 12 h light/dark cycle and given ad libitum access to water and food.

Photothrombotic Stroke

Targeted focal ischemic stroke in the distal branch of the MCA was induced using a modified version of the photothrombotic method (Watson, 1985). Animals were anaesthetized with isoflurane (2% for induction, 1.5% for maintenance) mixed with medical air (20% Oxygen, 80% Nitrogen) at a flow rate of 0.7L/min. Animals were kept on a heating pad with feedback from a rectal thermoprobe and temperature regulator to maintain a body temperature of 37°C. Ophthalmic liquid gel (Novartis) was placed on the eyes. A midline incision was made on the scalp and the skin was retracted. Connective tissue was removed and gelfoam soaked in ACSF was placed on the skull to permit visibility of the brain's surface vessels through the moist skull. The right middle cerebral artery was identified and a 0.5 mm diameter circle was thinned over the lateral extent of the artery with a high-speed dental drill. The area surrounding the thinned skull was covered with black permanent marker so that only the exposed small segment of the MCA was targeted. A hollow female luer connector (diameter 6 mm) was fixed to the skull surrounding the thinned circle with cyanoacrylate glue and dental cement. The

incision was closed around the connector with cyanoacrylate glue and the animals recovered under a heating lamp and were returned to their home cages. Twenty four hours later, 20 µl of mineral oil was pipetted onto the exposed skull inside the female luer connector to make the skull more transparent, and a fibre optic cable delivering green laser light (532 nm, 15.29 mW/mm^2, 1 mm diameter) with a male luer lock was fastened to the female luer connector. Mice received an injection of 1% rose bengal dye (110 mg/kg, i.p.) dissolved in ACSF and photoactivation began 2 minutes after injection. The animal was exposed to laser light for 60 min. Mice were placed in a clean cage and allowed to move freely during the procedure. For the anaesthetized group, animals were anaesthetized with isoflurane in medical air and kept on a heating pad with feedback from a rectal thermoprobe and temperature regulator to maintain a body temperature of 37°C. Photothrombosis was initiated exactly as described for the freely moving animals. After photothrombosis, all mice recovered under a heating lamp and were returned to their home cages. The overall success rate for stroke induction using this model was 87%.

Drug Delivery

To acutely block α4β2 nAChR after stroke, animals received an intraperitoneal injection of vehicle (0.9% sterile saline) or α4β2 nAChR-specific antagonist dihydro-beta-erythroidine hydrobromide (DHβE, Tocris Bioscience; 3 mg/kg dissolved in saline) 90 minutes or 3 hours after initiating photothrombosis.

Laser Doppler

Animals were prepared for targeted MCA photothrombotic stroke as described above. During the female luer connector implantation a second 1 mm circle was thinned 3.5 mm posterior to the targeted portion of the MCA using a high-speed dental drill. A 20-gauge

guide cannula (15mm long) was fixed to the skull over the circle using cyanoacrylate glue and dental cement. Before initiation of photothrombosis, a 0.5 mm plastic fibre optic probe connected to a laser Doppler blood flow monitor (Moor Instruments, moorVMS-LDF1; Wilmington, Delaware) was inserted into the guide cannula and glued to the thinned skull using cyanoacrylate glue. Baseline recordings were measured for 10 minutes before photothrombosis commenced and perfusion measurements were collected at 10 Hz continuously for up to 2.5 hours. Mice were injected with vehicle or DHβE 90 minutes following initiation of photoactivation.

Laser Doppler recordings were processed by importing data into IGOR Pro (Wavemetrics). Perfusion data were processed with a differentiation algorithm followed by manual thresholding and binomial smoothing (radius = 3) to help eliminate large amplitude movement induced spikes. Perfusion values for each experiment were generated by taking the average perfusion over a 10-minute period before the induction of stroke, before injection (see Fig. 5B "pre-inject") or 5-15 minutes after injection ("post-inject").

Physiological Monitoring

Blood collection was taken from the ventral artery of the tail in un-anaesthetized mice 30 minutes after administration of vehicle or DHβE. 95-150 µl samples were collected using heparinized capillary tubes. Blood samples were measured immediately after sample collection with an iSTAT-1 analyzer using CG8+ cartridges (Abbott Point of Care Inc., Princeton) in order to assess arterial pH, pCO_2, pO_2, HCO_3, glucose, hemoglobin, hematocrit, Na^+ and K^+ concentrations. Heart rate, breath rate, and oxygen

saturation were measured using a MouseOx pulse oximeter (Starr Life Sciences, Oakmont, PA).

Confocal Imaging

Two and 24 hours after initiating photothrombotic stroke, mice were anaesthetized with 1.5% isoflurane in medical air and injected with 250 µl of 4% Evans blue (Sigma Aldrich) dissolved in 0.9% sterile saline through the tail vein in order to visualize the thrombus in the distal middle cerebral artery. Mice were then decapitated and whole brains were extracted and post-fixed in 4% PFA overnight and then transferred to 0.1 M PBS solution.

Whole brains were imaged with a 4× objective (NA = 0.13) using an Olympus confocal microscope controlled by Fluoview software. High resolution image stacks were collected using 515 and 635 nm lasers to excite rose bengal and Evans blue fluorophores, respectively. Image stacks were collected using a Kalman filter (average of 2 images) in 25 µm z-steps at 640 × 640 pixels (5 µm/pixel) with a pixel dwell time of 4 µs. To verify a permanent occlusion in the MCA as well as quantify the extent of reperfusion, maximal intensity z-projections of each tiled image stack were produced and stitched together in Image J software (NIH, version 1.44d).

Histology

The whole brain was cut into 50 µm sections on a Leica vibratome in the coronal plane. To quantify infarct volume 24 hours after stroke, every third section was stained using 0.0001% Fluoro-Jade C (Millipore), a marker of dying cells and mounted onto glass slides. Wide-field epifluorescence images of serial sections were imaged with a 4× objective (NA = 0.13) using a GFP filter set (Semrock) on an Olympus microscope. All

infarcts were quantified using ImageJ software (NIH, version 1.44d). The area of infarction was measured in each section by a blind observer and infarct volume was calculated by summing up the infarct area for each section multiplied by the distance between sections (150 μm).

Statistics

A priori Analysis of Variance (ANOVA) and independent samples t-tests were used to analyze data for main effects and statistical significance. All p values ≤ 0.05 were considered statistically significant. Statistical analyses were conducted using SPSS 20 (SPSS Inc., Chicago, IL). Data are presented as mean ± SEM.

2.3 Results

To investigate α4β2 nAChR signalling as a modulator of ischemic damage, we performed two experiments that are summarized in Figure 2. The first aim was to determine if α4β2 nAChR antagonism would affect the severity of infarction in the immediate stages after ischemic stroke by measuring infarct volume in saline and DHβE-treated mice. The second experiment sought to understand the mechanism through which DHβE could act as a neuroprotectant. We assessed its role in collateral blood flow by quantifying the degree of reperfusion that is observed in the peri-infarct region.

Acute α4ß2 nAChR antagonism results in smaller infarcts

There were significant differences in infarct volume between animals treated with saline and DHβE at one day after stroke (Fig. 3). Awake animals treated with DHβE 90 minutes following induction (n=9) had smaller infarct volumes compared to saline controls (n=10) ($t_{(17)}$=2.84, p=0.01). However, anaesthetized animals treated with DHβE at 90 minutes (n=9) did not differ from anaesthetized saline controls (n=11) ($t_{(18)}$=0.84,

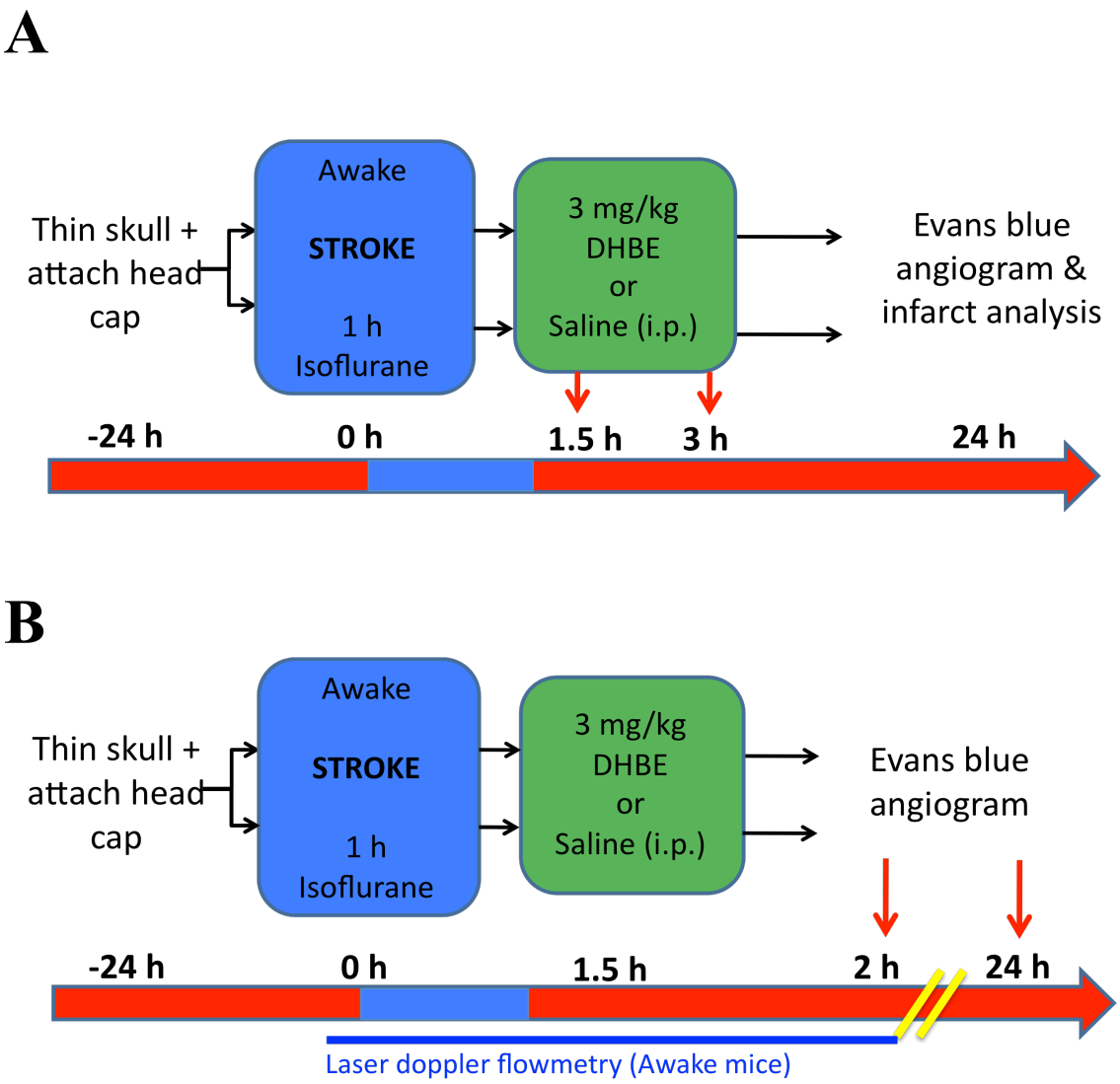

Figure 2. Summary of experiments studying the effect of DHβE on ischemic damage.

A) Diagram summarizing Experiment 1: investigating the effect of DHβE on infarct volume. **B)** Diagram summarizing Experiment 2: investigating the effect of DHβE on collateral blood flow.

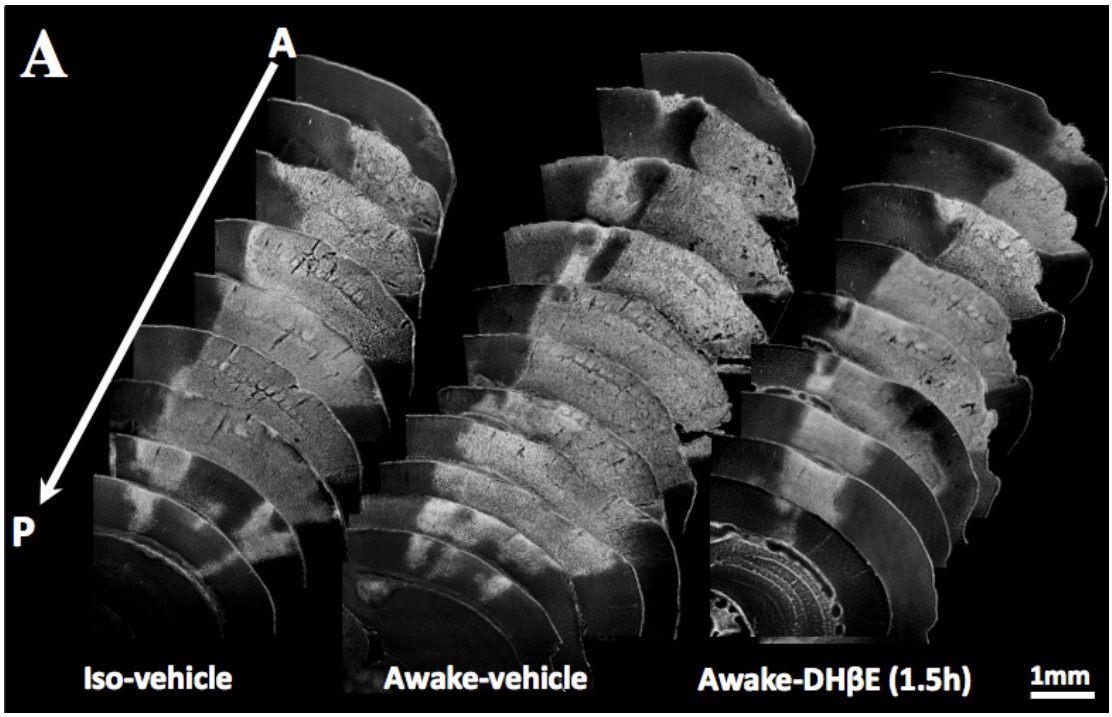

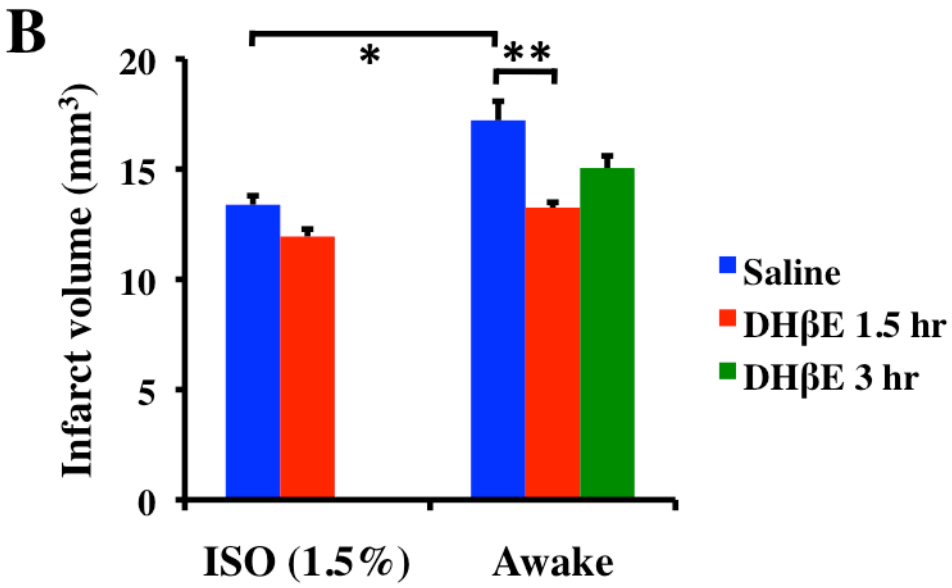

Figure 3. Acute α4ß2 nAChR antagonism results in smaller infarcts.

A) Representative Fluoro-jade C stained coronal sections of the stroke hemisphere in anaesthetized saline, awake saline, and awake DHßE-treated mice 24 hours after stroke. **B)** Histogram showing that DHßE significantly decreases infarct volume in awake mice at 1.5 hrs but not 3 hrs after stroke. Mice given strokes under isoflurane have significantly smaller infarcts than awake saline mice. Scale bar=1 mm. Data are mean ± SEM.

p=0.41). Awake saline animals had much larger infarcts than anaesthetized saline animals ($t_{(19)}$=2.53, p=0.02), which is expected because isoflurane has been described as a neuroprotectant in stroke models (Kapinya et al., 2002; Khatibi et al., 2011). Furthermore, the group of awake animals treated with DHβE 3 hours (n=11) after stroke induction showed a moderate decrease in infarct volume compared to awake controls but this effect failed to reach significance ($t_{(19)}$=1.43, p=0.17). These results suggest that early, but not delayed treatment with DHβE can salvage brain tissue after stroke.

DHβE does not protect the brain through a collateral flow mechanism

Animals were injected with Evans blue dye through the tail vein to image reperfusion of the MCA branches with confocal microscopy. Evans blue binds to plasma albumin, therefore areas of the vessel that fluoresce under confocal imaging correspond to blood flow while the absence of fluorescence in the vessels indicates no flow (Radius and Anderson, 1980). To quantify blood flow we measured the optical density of vessels downstream from the occluded branch. If DHβE at 90 minutes reduces infarct size one day after stroke through greater reperfusion, one would expect that animals treated with DHβE would show more blood flow closer to the occluded region. However, it appears that there was no effect of DHβE treatment on collateral blood flow seen at 24 hours after stroke in awake animals (Fig. 4C; $F_{(1,13)}$=0.01, p=0.93). There were also no differences between anaesthetized mice treated with DHβE relative to saline controls (Fig. 4C; $F_{(1,13)}$=2.98, p=0.11). Awake saline animals did not show any differences in collateral flow compared to anaesthetized saline animals (Fig. 4C; $F_{(1,16)}$=2.38 p=0.14). There were also no significant differences between awake mice treated with DHβE and saline seen at

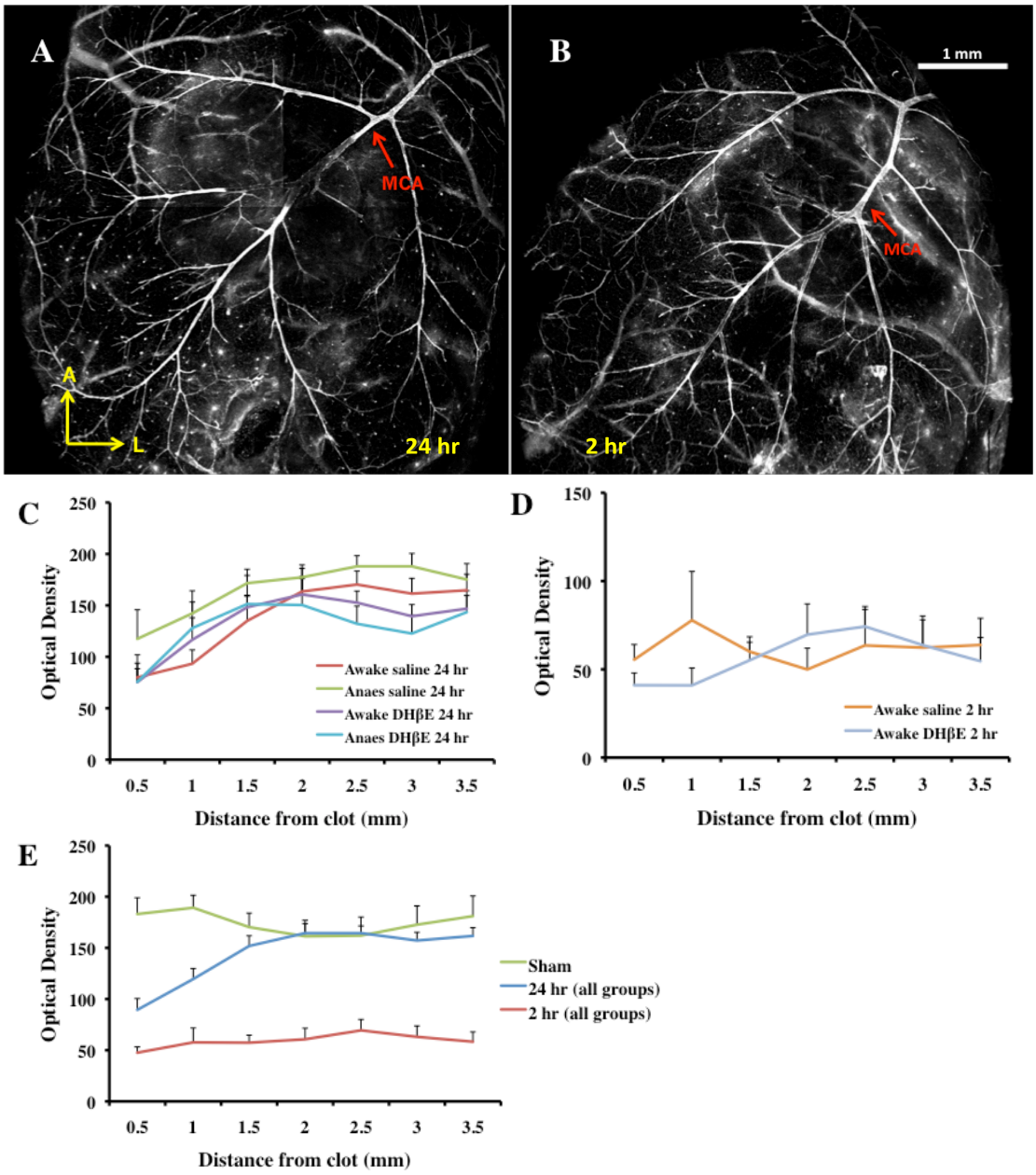

Figure 4. DHβE does not induce neuroprotection by altering collateral blood flow.

A) Representative Evans blue surface vessel angiogram taken 24 hours after stroke **B)** Representative Evans blue surface vessel angiogram taken 2 hours after stroke. **C)** Line graph showing that isoflurane or drug treatment has no effect on the blood flow of vessels downstream from the clot 24 hours after stroke. **D)** Line graph showing that drug treatment has no effect on blood flow of vessels downstream from the clot 2 hours after stroke. **E)** Line graph showing that at 24 hours after stroke there is greater blood flow in downstream vessels compared to at 2 hours after stroke. Scale bar=1 mm. Data are mean ± SEM.

2 hours after stroke (Fig. 4D; $F_{(1,9)}$=0.14, p=0.72). There does appear to be a correlation between collateral blood flow and time after stroke (Fig. 4E). Two hours after the beginning of stroke induction animals showed lower levels of reperfusion while animals given 24 hours to recover had values approaching those of sham controls ($F_{(1,39)}$=43.98, p<0.01). Overall, these data indicate that DHβE does not exert its neuroprotective effects through increased collateral blood flow.

Laser Doppler flowmetry was used to measure perfusion levels in the cortical penumbra during stroke induction in freely moving mice. Following initiation of photothrombosis, both groups showed a progressive drop in blood flow that stabilized by 90 minutes. There were no differences in the average percent change in blood flow in penumbral regions compared to baseline levels before and after injection between vehicle- (n=4) or DHβE-treated (n=5) mice (Fig 5B; $t_{(7)}$=0.62, p=0.55), further demonstrating that DHβE does not change blood flow in the penumbra.

Physiological variables taken from un-anaesthetized mice treated with vehicle (n=3) or DHβE (n=3) are shown in Table 1. No differences were observed in arterial pH, pCO_2, pO_2, HCO_3, glucose, hemoglobin, hematocrit, Na^+ and K^+ concentrations, oxygen saturation (SpO_2), heart rate, and breath rate with injection of saline or 3 mg/kg DHβE (all *p*-values=0.09-0.77).

2.4 Discussion

We explored the use of DHβE as a neuroprotectant following ischemic stroke induced in freely moving and anaesthetized mice. Treatment with DHβE at 90 minutes but not 3 hours after injection significantly reduced ischemic damage. Of note, this effect was only found in awake mice, given that infarct volumes in anaesthetized mice treated with DHβE

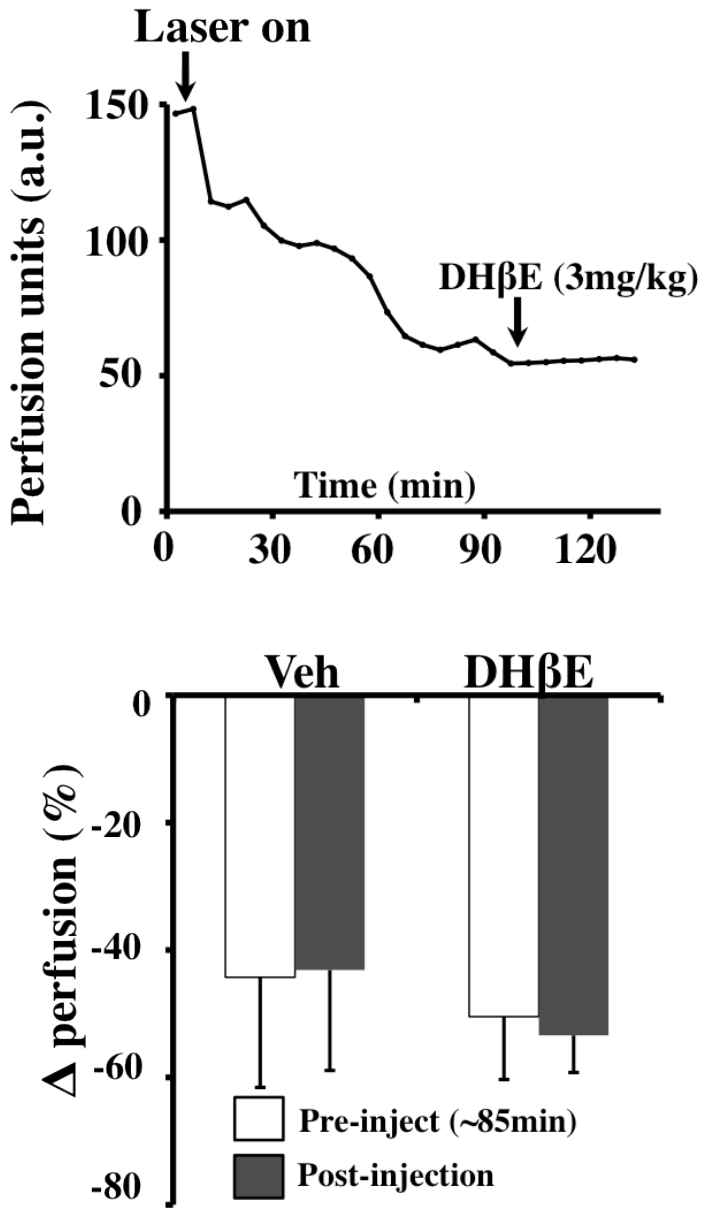

Figure 5. Laser Doppler flowmetry reveals no effect of DHβE treatment on blood perfusion during stroke.

A) Representative laser Doppler recording of blood flow in penumbral cortical regions in awake mice who were treated with DHβE 1.5 hrs after start of induction. Each data point represents a 5 min average of perfusion. There is a progressive drop of blood flow with the start of laser induced photothrombosis and DHβE has no effect on cortical perfusion. **B)** Histogram showing the average percent change in penumbral blood flow relative to baseline perfusion in awake animals treated with vehicle or DHβE. Neither treatment altered cortical blood perfusion in the penumbra relative to pre-injection values. Data are mean ± SEM.

Table 1. Physiological variables for drug experiments.

	Awake - vehicle	Awake - DHβE
pH	7.35 ± 0.04	7.32 ± 0.04
pCO_2 (mmHg)	38.3 ± 0.52	37.6 ± 0.87
pO_2 (mmHg)	89.6 ± 3.8	95.3 ± 7.8
HCO_3 (mmol/L)	21.2 ± 1.9	19.3 ± 1.3
Na (mmol/L)	146 ± 1.2	148 ± 0.3
K (mmol/L)	6.2 ± 0.3	5.6 ± 0.2
Glucose (mg/dL)	240 ± 26	204 ± 38
Hematocrit (%)	46.3 ± 2.3	45.2 ± 2.0
SpO_2 (%)	94.2 ± 1.4	92.0 ± 1.7
Heart Rate (bpm)	671 ± 60	702 ± 13
Breath Rate (brpm)	151 ± 16	183 ± 16

Arterial blood was measured in un-anaesthetized mice 30 minutes after administration of vehicle or DHβE. There are no differences in any physiological variables between groups. Data are mean ± SEM.

or saline treatment did not differ. However, DHβE did not appear to affect reperfusion of blood flow during or after ischemic stroke and did not affect physiological variables half an hour after injection. Based on our data, it is evident that blocking α4ß2 nAChRs can be neuroprotective when given at an early time point. However, the mechanism underlying this effect is still unclear.

Nicotinic receptor activation has shown neuroprotective effects in studies examining processes involved in the ischemic cascade. Glutamate-mediated excitotoxicity is involved in inducing cell death during ischemic insult. Excitotoxicity has been shown to be reduced by cholinergic signalling through α4ß2 nAChRs, an effect that is nullified with pre-treatment with DHßE (Akaike et al., 1994; Stevens et al., 2003; Takada et al., 2003; Thompson et al., 2006). However, these studies looked at cell cultures that were pre-incubated with nAChR agonists or acetylcholinesterase (AChE) inhibitors before glutamate stimulation, and demonstrated a beneficial effect of nAChR activation only

with prior but not simultaneous exposure of drug treatment to the excitotoxic insult. It has also been established that nicotinic receptor activation can elicit harmful effects to the central nervous system in mechanisms relevant to ischemia. Wang et al., (1997) have shown that nicotine treatment for two weeks diminished the readily available pool of endogenous tissue plasminogen activator (tPA), an enzyme that promotes fibrinolytic and thrombolytic activity, in the microvasculature. Furthermore, increased production of plasminogen activator inhibitor type 1 (PAI-1), which binds to tPA to render it inactive, is observed in human endothelial cells following treatment with nicotine at doses similar to those seen in smokers (Zidovetzki et al., 1999). Work from the Wetscher lab (1995a, 1995b) describes elevated production of reactive oxygen species and enhanced lipid peroxidation activity, both processes which are prominent in inducing ischemic damage, in esophageal mucosa and pancreatic cells when treated with nicotine. Indeed, nicotine appears to cause oxidative stress in a dose-dependent manner, as excessive activation of nAChRs increases lipid peroxidation and reduces cell viability (Guan et al., 2003). Interestingly, very low doses of nicotine in the same experiment produced an antioxidant effect against activation of a free radical inducer, suggesting that an optimal level of nicotinic receptor activation exists for neuroprotection. Finally, blood brain barrier integrity is compromised in ischemic conditions, a phenomenon that is exacerbated further with exposure to nicotine and cotinine, a metabolite of nicotine, and is mediated by nAChRs containing α7 and ß2 subunits (Abbruscato et al., 2002; Hawkins et al., 2004, 2005). The BBB is an important modulator of CNS health and normally prevents the entry of foreign and harmful substances into the brain parenchyma. Nicotine and cotinine appear to reduce the health of endothelial cells and alter the expression of proteins that

regulate the integrity of tight junctions in the BBB (Hawkins et al., 2004). It is possible that ischemia induces heightened nAChR activation that is similar to what is observed in these studies. Currently there is a dearth of literature on the effects of nAChR antagonist treatment alone after stroke, but given the amount of evidence showing that nAChR agonism can activate damaging processes in the brain, the neuroprotective effect of DHßE after stroke is certainly plausible.

The current literature shows that nicotine application appears to have neuroprotective as well as neurodegenerative outcomes depending on dosage and time of administration. An optimal level of nicotinic receptor activity may exist for stroke neuroprotection, but this level may be exceeded in ischemic conditions. Alterations in nicotinic receptor signalling following stroke are poorly understood. The mechanism behind the action of DHßE in stroke pathophysiology is still speculative but, based on our data, it does not involve changes in reperfusion and collateral flow. While we predicted that changes in nAChR signalling during stroke would alter α4ß2 nAChR-mediated vasodilation as seen with chronic, high-dose nicotine treatment, it appears that DHßE did not elicit any changes in collateral flow (Uchida et al., 2009). Considering the variety of processes that nicotinic acetylcholine receptors are involved in with respect to ischemia, this result is not completely unexpected, as there are many mechanistic possibilities in which DHßE may be involved including interactions that decrease BBB permeability and ROS production. It is well established that nicotine also increases energy metabolism in chronic smokers, and reducing energy requirements of vulnerable cells in the penumbra might be a critical part of DHßE involvement (Domino et al., 2000; Pettegrew et al.,

2001; Shameem and Patel, 2012). There are many existing possibilities that will need to be explored in future studies.

These experiments are the first to investigate neuroprotection in an awake model of stroke. Our study has also demonstrated that isoflurane promotes neuroprotection after stroke, and this effect masks the effect of DHβE in anaesthetized animals. This is important to note because many studies looking at animal models of stroke use volatile anaesthetics during stroke induction. Our results present a confound in neuroprotection studies that may lead researchers to miss potential therapies in basic and preclinical research.

Due to the novel nature of this study, there are many unresolved issues that need to be investigated in future research. It is important to explore whether DHßE-mediated neuroprotection is associated with long-term improvement. Since our experiments only examined lesion size acutely after stroke, it is uncertain whether DHßE confers permanent neuroprotection or if treatment merely delays inevitable damage to a later time point. It will also be important to examine how the reduction in stroke size observed acutely after DHßE treatment affects neurological and behavioural performance in order to establish the potential of this drug as a clinical neuroprotectant. Moreover, it is imperative to determine an optimal dose and time point at which to administer DHßE. Due to the nature of ischemia in humans, many patients are unable to receive pharmacological treatment during a time window when neuroprotectants are efficacious, so it is crucial to establish the maximum time after stroke at which DHßE is still effective. In summary, blocking nicotinic acetylcholine receptor activity following ischemia promotes neuroprotection by attenuating tissue damage, and reveals a novel

mechanism that will be crucial to investigate as a potential therapy in the acute phase of stroke recovery.

Chapter 3: Chronic Recovery Following Ischemic Stroke

3.1 Introduction

There is a wide body of research that investigates mechanisms of stroke recovery in order to improve the outcome of patients. Yet currently, recombinant tissue plasminogen activator (rtPA) is the only FDA-approved drug treatment for reperfusion of brain tissue (Moskowitz et al., 2010). The caveat with rtPA is that it must be used within 3-4.5 hours after the onset of symptoms, or else the risk of causing additional hemorrhage is increased (NINDS, 1995; Clark et al., 1999; Sahlas et al., 2013). Unfortunately, the majority of stroke patients do not access treatment within this crucial window and only 8% percent of individuals who were otherwise eligible for rtPA treatment sought treatment in time to receive the drug (Lloyd-Jones et al., 2010). Therefore, significant effort must be placed on developing pharmacological therapies that can be implemented at later stages of stroke recovery (>4.5 hours) which would benefit a much larger segment of the clinical population.

A key feature of stroke pathology is the disruption of brain excitability, and there is evidence that ischemia leads to excessive GABAergic inhibition in peri-infarct regions. (Clarkson et al., 2010). Targeting this network to reduce inhibition improved performance in paw and foot function in mice (Clarkson et al., 2010). Our lab has demonstrated that α4ß2 nAChRs are expressed on GABAergic cell bodies and have a profound influence on cortical excitability (Brown et al., 2012). Activating α4ß2 nAChRs *in vivo* can suppress synaptic activity in the somatosensory cortex, while applying an α4ß2 nAChR antagonist enhances whisker evoked sensory responses (Brown et al.,

2012). Therefore, it is possible that α4ß2 nAChRs can improve cortical excitability after stroke by targeting GABAergic systems.

Objective and Hypothesis

The objective of this study was to elucidate the role of α4ß2 nAChRs on long-term recovery of function after stroke. We hypothesized that stroke-related changes in α4ß2 nAChR mediated signalling is driving the excessive GABAergic neurotransmission in peri-infarct regions after stroke. To test this hypothesis, we induced ischemic stroke in the right forelimb somatosensory cortex (FLS1) and characterized the expression of α4ß2 nAChRs on GABAergic cells using confocal microscopy. This experiment clearly showed that α4ß2 nAChRs were upregulated in peri-infarct cortex. Next, we examined whether that chronic infusion of DHβE after stroke could affect the recovery of forelimb function. Lastly, once behavioural testing was completed, mice underwent voltage-sensitive dye (VSD) imaging to verify whether pharmacological antagonism of α4ß2 nAChRs promoted the recovery and re-organization of forelimb sensory maps in the cerebral cortex.

3.2 Methods

Animals

Adult (2-5 months old) male (n=32) and female (n=6) α4-YFP knock-in mice with C57BL/6J background were used (Nashmi et al., 2007). All experiments were conducted in accordance with guidelines set by the Canadian Council for Animal Care.

Photothrombotic Stroke

Focal ischemic stroke of the right forelimb somatosensory cortex was induced with the photothrombotic method (Watson et al., 1985; Brown et al., 2007). Animals were

anaesthetized and prepared for surgery as described in section 2.2 for the single-vessel occlusion experiments. A midline incision was made on the scalp and the skin was retracted with two microclamps. Connective tissue was removed from the skull and a 1.5 x 1.5 mm box was thinned to ~50% of original thickness over the forelimb region of cortex (~2-4 mm lateral; -1 to 1 mm anterior to bregma) with a high-speed dental drill. To initiate photothrombosis, mice received an injection of 1% rose bengal dye (110 mg/kg, i.p., Sigma Aldrich) dissolved in HEPES-buffered artificial cerebrospinal fluid (ACSF) and the thinned region of skull was exposed to a collimated green laser light (532 nm, 21 mW) for 15 min. Controls received a sham surgery in which animals were treated identically with the omission of rose bengal injection. Following stroke induction the scalp was sutured (braided silk, reverse cutting 45 cm sterile, Ethicon 62G) and the knots were covered with cyanoacrylate glue to prevent cagemates from removing the sutures during healing. After surgery, mice recovered under a heating lamp and returned to their home cages.

Drug Delivery

To chronically block α4ß2 nAChR *in vivo* after stroke, a mini-osmotic pump (Alzet, Model 2001; Cupertino, CA) filled with 0.9% sterile saline (control) or competitive antagonist DHβE (Tocris Bioscience) dissolved in saline was implanted subcutaneously in the thoracic-lumbar region of the back. Mice were anaesthetized with isoflurane and prepared for surgery as described in the photothrombotic procedure. A 1.5 cm midline incision was made in the mid-thoracic area. A pair of small, closed scissors was inserted under the skin to bluntly dissect a subcutaneous pocket. The pump was inserted into the pocket and sutured. DHβE was infused subcutaneously over 6 weeks at a dose of 1

mg/kg/h at a flow rate of 1 μl/hr. Due to the solubility of the drug and type of pumps available, mini-pumps were replaced each week. At 6 weeks after stroke, mini-pumps were removed.

Behavioural Testing

The adhesive tape removal test and ladder rung walking test were used to evaluate sensorimotor function of the forepaw. The tape removal test is sensitive to changes in forepaw sensation after stroke while the ladder rung walking test is able to measure impairments in forelimb use and has been used to track motor recovery following stroke (Metz and Whishaw, 2002; Schallert, 2006; Shanina et al., 2006; Tennant and Jones, 2009). Training and baseline sessions were administered for 2 weeks before stroke and testing was administered weekly for 10 weeks afterward. Tests were performed as previously described in our lab (Sweetnam et al., 2012). In the tape removal test, during each trial, a 5 mm diameter circular piece of tape was applied to the ventral side of each forepaw. Mice were then placed in a glass cylinder and filmed with a Logitech webcam until the tape was removed from each paw, to a maximum of 60 seconds. Three trials were performed in each session, and a blinded observer analyzed videos to measure the latency of tape removal for each paw. For the ladder rung walking test, mice were videotaped as they walked across an elevated horizontal ladder with 1 mm diameter rungs randomly spaced 1 or 2 cm apart. Frame by frame analysis of forepaw placements on the rungs was based on previously defined criteria (Metz and Whishaw, 2002; Sweetnam et al., 2012). Forepaw placements were scored as “correct” (forepaw is centered on the rung), “partial” (forepaw partially grasping rung) or “slip/miss.” Behavioural data was averaged in 2-week bins.

Voltage-sensitive Dye Imaging

Mice were anaesthetized with 1-1.5% isoflurane mixed with medical air (2% for induction). Mice were secured into a stereotaxic frame and were kept on a heating pad with feedback from a rectal thermoprobe and temperature regulator to maintain a body temperature of 37°C. Opthalmic liquid gel (Novartis) was placed on the eyes. Animals received 0.15 ml/h of 20 mM glucose (i.p.) dissolved in ACSF while under anaesthesia to maintain adequate hydration. A midline incision was made in the scalp and a metal plate was secured onto the skull with cyanoacrylate glue and dental cement and fastened onto the surgery stage in order to stabilize the head during imaging. A portion of the temporalis muscle was teased back to expose the lateral side of the skull, and a 5 mm medial-lateral x 7 mm anterior-posterior area of the skull overlying the right hemisphere was drilled and removed. During drilling, the skull was intermittently bathed in ACSF to keep it moist and the brain cool. When the brain was exposed, gelfoam soaked in ACSF was used to keep the brain surface moist. Dura was carefully removed using fine-tipped forceps. Voltage-sensitive dye RH1692 dissolved in ACSF (Optical Imaging, 1 mg/ml passed through 0.22 μm polyvinylidene fluoride syringe filter) was applied to the brain for 60-75 min, and refreshed halfway through this period. Following incubation, the brain was rinsed thoroughly with ACSF, covered with 1.3% low-melt agarose dissolved in ACSF and sealed with a glass coverslip.

For voltage-sensitive dye (VSD) imaging, 12-bit image frames (184x124 pixels) were captured every 4ms using a MiCAM02 HR high speed camera coupled to Brain Vision imaging software version 8.19. The dye was excited with Luxeon K2 red LED (627nm, ~20mW at back aperture) that was passed through a Cy5 filter cube (exciter: 605-650nm, emitter: 670-720nm). Red light was focused 200-300μm below the cortical surface using

an Olympus XFluor 2X objective (NA=0.14). The forepaw was mechanically stimulated by a computer-controlled piezoelectric wafer (Q220-AY-203YB, Piezo Systems; ~300μm deflection in the caudal-rostral plane) attached 7 mm away from the forepaw by gluing the paw to a pencil lead that was attached to the piezoelectric wafer. During each trial, images were collected 250ms before a single 5ms deflection of the forepaw (or not for null stimulation trials) and then 550ms afterwards. This process was repeated 12 times with approximately 10-second interval between trials. To correct for dye bleaching, stimulation trials were divided by null stimulation trials. VSD images are presented as the percent change in VSD fluorescence ($\Delta F/F_o$) by dividing frames collected after stimulation by the average of those taken 100ms before stimulation. Montages of cortical responses were generated by mean filtering $\Delta F/F_o$ image stacks (radius=2) and then binning 2 frames in time (hence 8ms between each image). The amplitudes of cortical depolarizations were expressed as the percentage change in VSD signal ($\Delta F/F_o$) relative to baseline fluorescence. Using Image J software, forelimb-evoked cortical responses were quantified by placing a circular region of interest (440 μm diameter) over the center of the FLS1, HLS1, M1, FLS2, or HLS2 cortex. After stroke, the FLS1 was defined as the remaining piece of forelimb cortex that showed the shortest latency to respond next to the stroke, typically immediately below or medial to the center of the original FLS1 region. The peak amplitude, time to peak amplitude, and half-width (i.e. duration) of VSD signals in the first 250 ms after stimulation were measured with Clampfit 9.0 software (Molecular Devices).

Histology

Mice were overdosed with sodium pentobarbital anaesthetic and transcardially perfused with 9 ml of phosphate buffered saline (PBS, 0.1 M) followed by 9 ml of 4% paraformaldehyde (PFA). Whole brains were postfixed in 4% PFA for 3-5 h and then transferred to 30% sucrose solution in order to cryoprotect the brains. All brain sections were cut at 50 μm around the lesion site on a Leica vibratome in the coronal plane.

For confocal imaging, sections from α4-YFP mice were incubated overnight at room temperature in PBS containing a single primary antibody for rabbit anti-GABA (1:1000, Sigma). Sections were then washed in PBS and then incubated for 4 h at room temperature with Cy5-conjugated donkey anti-rabbit (1:500, Jackson Immunoresearch Laboratories). After incubation, sections were washed in PBS, mounted on glass slides and coverslipped with fluorescent mounting media (Fluoromount-G, Southern Biotech).

Sections were imaged with a 60× oil objective (NA = 1.35) using an Olympus confocal microscope controlled by Fluoview software. High resolution image stacks were collected sequentially using 488 and 635 nm lasers to excite YFP and Cy5 fluorophores, respectively. Image stacks were collected in 0.5 μm z-steps at 12 bit intensity resolution at 1024 × 1024 pixels (0.065 μm/pixel) with a pixel dwell time of 4 μs. To quantify changes in α4-YFP expression (note: α4-YFP has a punctate appearance) after stroke, 20 images, each with an area of 10,231.3 μm^2, were analyzed. Therefore, the volume of tissue that puncta were quantified from was typically 102,313.2 μm^3. To remove background fluorescence, a duplicate of each image projection was smoothed (mean filter of 80) and subtracted from the original image. The number of α4-YFP puncta was quantified using a particle analysis macro in NIH ImageJ (version 1.44d). For

determining α4-YFP colocalization with markers of GABA cells, images in each channel were manually thresholded and then overlaid.

To quantify infarct volume, every third section (150 μm apart) was stained using cresyl violet and mounted onto glass slides. Serial sections were imaged with a 4× objective (NA = 0.13) under bright-field illumination. All infarcts were quantified using NIH ImageJ software (version 1.44d). The area of infarction was determined to be the area with abnormal nissl substance staining (uneven clusters and lack of staining). The infarct was measured in each section by a blind observer and an estimate of volume was calculated by summing up the infarct area for each section multiplied by the distance between sections.

Statistics

A priori Analysis of Variance (ANOVA) tests were used to analyze the behavioral data and a priori student's t-tests (independent samples and paired samples) were used to analyze the confocal imaging, VSD imaging, and infarct data for main effects and statistical significance. All p values ≤ 0.05 were considered statistically significant. Statistical analyses were conducted using SPSS 20 (SPSS Inc., Chicago, IL). Data are presented as mean ± SEM.

3.3 Results

α4ß2 nAChRs are upregulated in the peri-infarct cortex after stroke

Confocal imaging was used to quantify α4-YFP puncta in cortical layers 2/3 one week after stroke. There were significant differences between stroke animals (n=11) and controls (n=5) in α4-YFP puncta expression (Fig. 6). Stroke led to significantly greater levels of α4-YFP puncta in the peri-infarct region compared to the contralateral homotopic cortex ($t_{(10)}=3.72$, $p<0.01$) or sham control animals ($t_{(14)}=3.59$, $p=0.03$). The

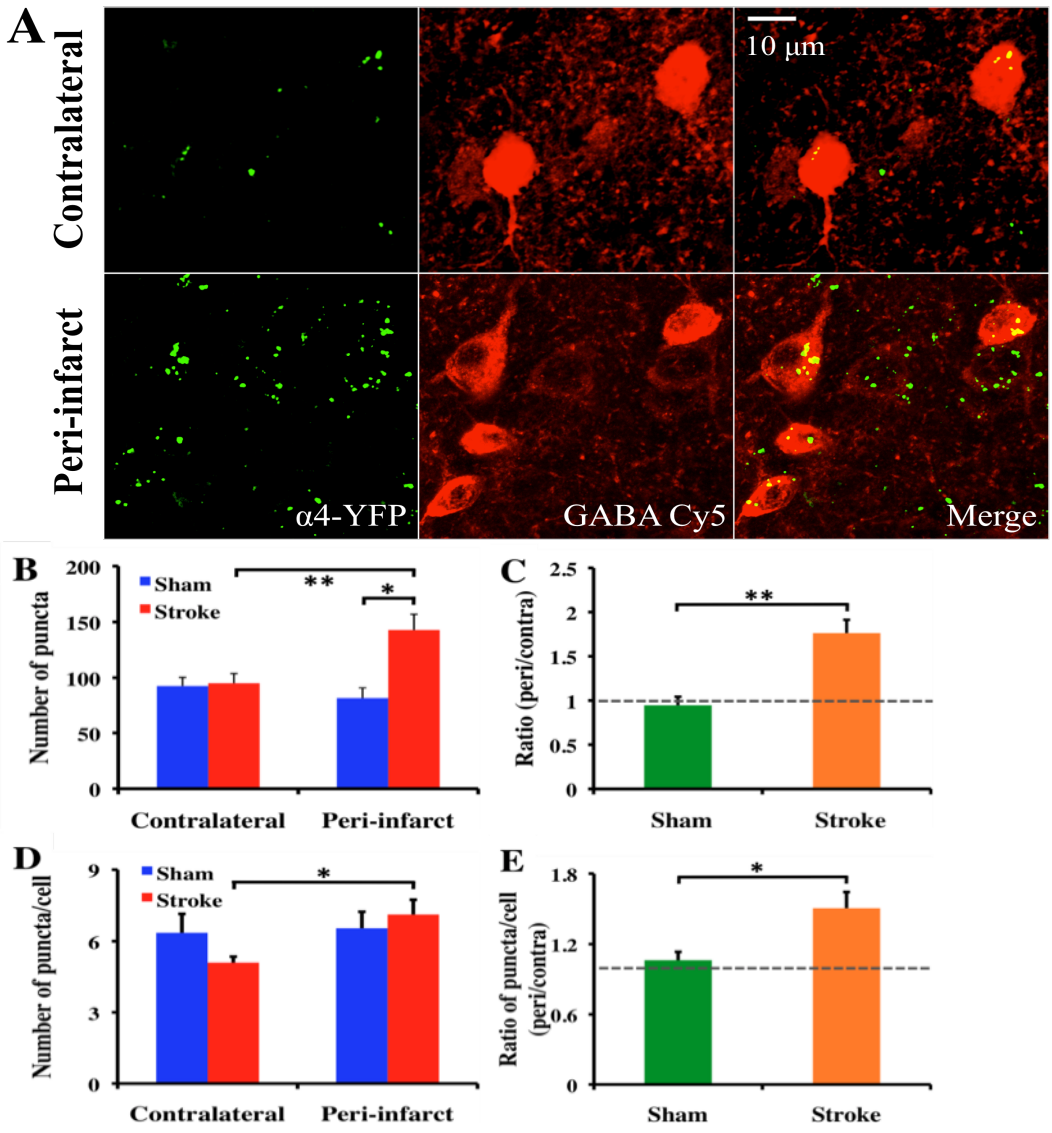

Figure 6. α4ß2 nAChR puncta are upregulated in the peri-infarct cortex after stroke.

A) High-magnification confocal images (60× objective, NA=1.35) showing that α4-YFP puncta were more highly expressed on GABAergic neurons in the peri-infarct cortex than in the contralateral cortex after stroke. **B)** Histogram showing that the overall α4-YFP puncta expression in the peri-infarct hemisphere was higher relative to the contralesional hemisphere in stroke animals, but there were no differences in sham animals. **C)** Histogram showing the ratio of hemisphere differences of total puncta in stroke and sham animals. **D)** Histogram showing that α4-YFP puncta expression on GABAergic cells in the peri-infarct was higher relative to the contralesional hemisphere in stroke animals but not in sham animals. **E)** Histogram showing the ratio of hemispheric differences of puncta per cell in stroke and sham animals. Data are mean ± SEM.

ratio of α4-YFP puncta in the peri-infarct cortex compared to the contralateral side was greater in stroke animals relative to sham controls (Fig. 6C; $t_{(14)}$=3.48, p<0.01). There were no differences in α4-YFP expression in the contralateral (undamaged) hemisphere between stroke and sham animals (Fig. 6B; $t_{(14)}$=0.18, p=0.86). There were also no differences between the peri-infarct region and contralateral hemisphere within sham animals (Fig. 6B; $t_{(4)}$=0.95, p=0.36). These data show that stroke leads to an upregulation of α4-YFP puncta expression in the peri-infarct region but not in the contralateral hemisphere.

α4ß2 nAChRs are normally expressed on excitatory and inhibitory neurons, so tissue was stained for GABAergic neurons to investigate if stroke induced an upregulation of receptors specifically on GABAergic cells. Stroke mice (n=6) showed greater expression of α4-YFP puncta on GABAergic cells in the peri-infarct cortex compared to the contralesional side (Fig. 6D; $t_{(5)}$=3.51, p=0.02). In sham animals (n=4), there were no differences in the number of α4-YFP puncta on GABAergic neurons between both hemispheres (Fig. 6D; $t_{(3)}$=0.40, p=0.72). Stroke increased the ratio of α4-YFP puncta per GABAergic cell in the peri-infarct cortex compared to the contralateral homotopic cortex (Fig. 6E; $t_{(8)}$=2.41, p=0.04). Overall, these results indicate that stroke upregulates α4-YFP puncta expression on GABAergic neurons.

Chronic α4ß2 nAChR antagonism does not improve functional recovery from stroke

Previous research has indicated that targeting GABA-mediated excessive inhibition after stroke is a crucial factor in improving forelimb function in mice (Clarkson et al., 2010). Therefore, we investigated the effects of chronic α4ß2 nAChR blockade with the α4ß2 receptor-specific antagonist DHβE (1 mg/kg/hr) on recovery of forepaw function.

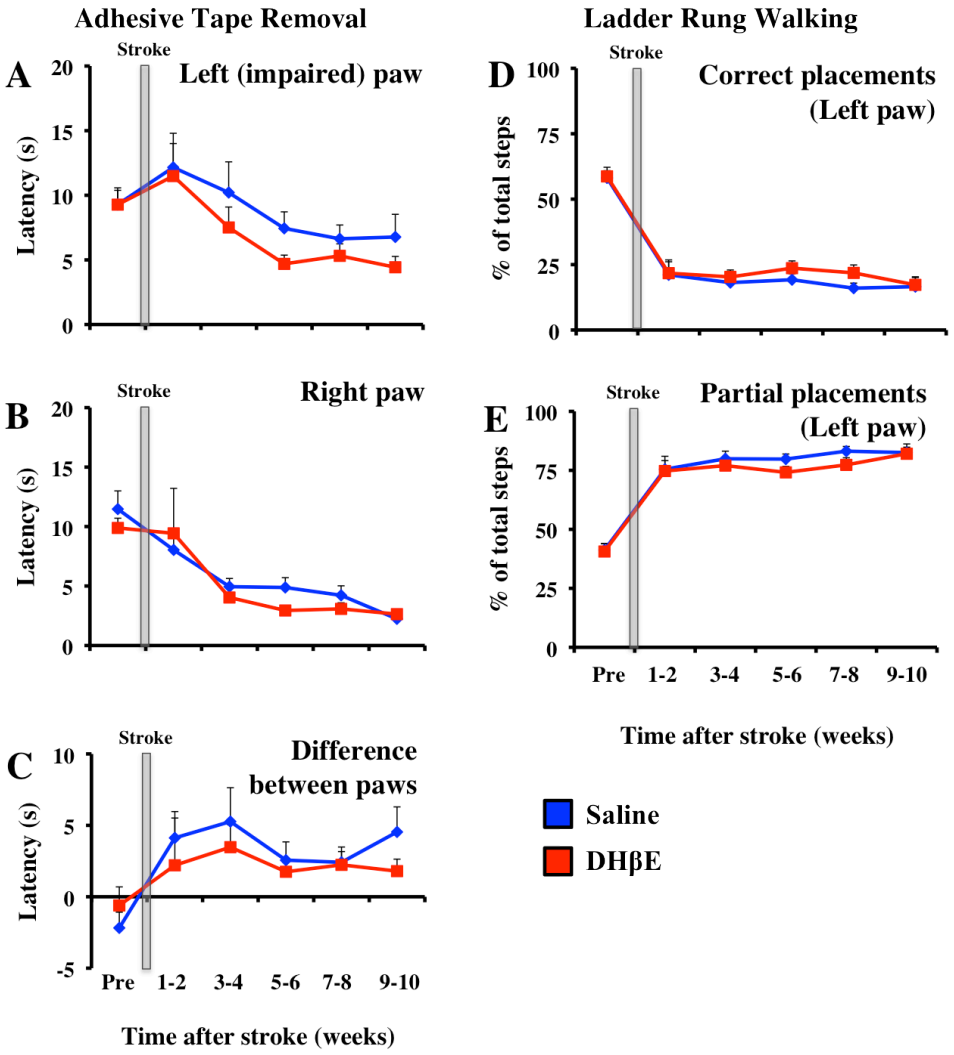

Figure 7. Long-term DHßE treatment does not improve behavioural recovery.

Animals infused with DHßE (1 mg/kg/hr) for 6 weeks following stroke showed no differences in behavioural improvement relative to saline controls. **A-C)** Data from the adhesive tape removal test. **A)** Line graph showing the latency to remove tape from the left (impaired) paw after stroke. There was no effect of DHßE on removal latency. **B)** Line graph showing the latency to remove tape from the right (unaffected) paw after stroke. There was no effect of stroke or drug treatment on the right paw. **C)** Line graph showing the differences in latency to remove tape between paws (left paw–right paw). There was no difference between saline and DHßE groups. **D-E)** Data from the ladder rung walking test. **D)** Line graph showing the number of correct placements in the left (impaired) paw after stroke. There were no differences between groups. **E)** Line graph showing the number of partial placements in the left paw after stroke. The incidence of partial placements did not differ between groups. Data are mean ± SEM.

In the adhesive tape removal tests, both saline (n=12) and DHβE-treated (n=10) groups showed a trend towards increased tape removal latencies on the left impaired forepaw 1-2 weeks after stroke, however this did not reach significance (Fig. 7A). Analysis of latencies across all time points revealed no difference between saline and DHβE-treated animals ($F_{(1,20)}$=1.22, p=0.28). As expected, there were no differences between groups in the unaffected right paw (Fig. 7B; $F_{(1,20)}$=0.56, p=0.46).

One caveat of our quantification of latencies (i.e. the number of seconds to remove tape once placed in the cylinder) is that subtle differences in mouse attention, anxiety and fear (manifested as freezing) could artificially increase latency scores. Therefore, we normalized the measurements by taking the difference in the time it took to remove tape from the left (impaired) paw relative to the right (unaffected) forepaw. Saline controls showed significantly increased difference scores after stroke at 1-2 weeks compared to baseline (Fig. 7C; $t_{(11)}$=5.61, p<0.01). DHßE-treated mice showed a trend towards increased difference scores after stroke at 1-2 weeks relative to baseline levels but this did not reach significance (Fig. 7C; $t_{(9)}$=1.72, p=0.12). This asymmetry in forelimb ability persisted throughout later weeks, but there were still no significant differences between groups ($F_{(1,20)}$=0.66, p=0.43). From these results, it appears that chronic DHßE treatment was not sufficient to promote recovery of forepaw sensation after stroke.

The ladder rung walking test measures limb placement and coordination and is sensitive to forelimb impairments resulting from unilateral stroke in rodents (Metz and Whishaw, 2002). After stroke, both groups showed impairment with a significant decrease in correct placements after stroke (Fig. 7D; $F_{(5,100)}$=79.02, p<0.01) and an increase in partial (incomplete) forepaw placements in the left (impaired) paw (Fig.

5E;$F_{(5,100)}$=77.09, p<0.01). Similar to the adhesive tape removal test, there was no difference between saline and DHßE groups on the ladder task in the impaired left paw on the incidence of correct placements (Fig. 7E; $F_{(1,20)}$=1.00, p=0.33) or partial forepaw placements (Fig. 7E; $F_{(1,20)}$=1.02, p=0.32). The right paw did not show any deficits at 1-2 weeks after stroke on the incidence of correct ($t_{(24)}$=0.12, p=0.91) and partial placements ($t_{(24)}$=0.32, p=0.75). Together, our behavioural data suggest that chronic DHßE treatment at a dose of 1 mg/kg/hr dose not improve the recovery of sensorimotor coordination.

Blocking α4ß2 nAChRs does not affect cortical responsiveness

Although chronic DHßE treatment failed to induce any obvious improvements in behavioural outcome of DHßE-treated animals, it is important to determine whether or not this is also represented in the cortical activation patterns of stroke-affected areas. After mice recovered for 14 weeks after ischemic stroke in the FLS1 cortex, we used voltage-sensitive dye (VSD) imaging to measure cortical responses to forelimb stimulation. A 5 ms tap on the forelimb elicited depolarizations in both the FLS1 and FLS2 that peaked at 18-21 ms after stimulation in mice given sham surgery (n=5) (Table 2). As previously shown, depolarizations arose from the FLS1 cortex and spread throughout adjacent areas (Brown et al., 2009; Sweetnam et al., 2012). At 14 weeks after stroke, there were responses to forelimb stimulation in the remaining portion of FLS1 and also posterior to the infarct area in the HLS1 region (Fig. 8).There were no differences between saline (n=5) and DHßE-treated (n=6) groups in the average peak amplitude, time to peak, and duration of cortical responses in all primary and secondary sensorimotor regions that were quantified (Fig. 8, Tables 2-4; all *p*-values=0.06-0.94). There was a trend towards smaller peak responses in the FLS1 region in stroke groups relative to

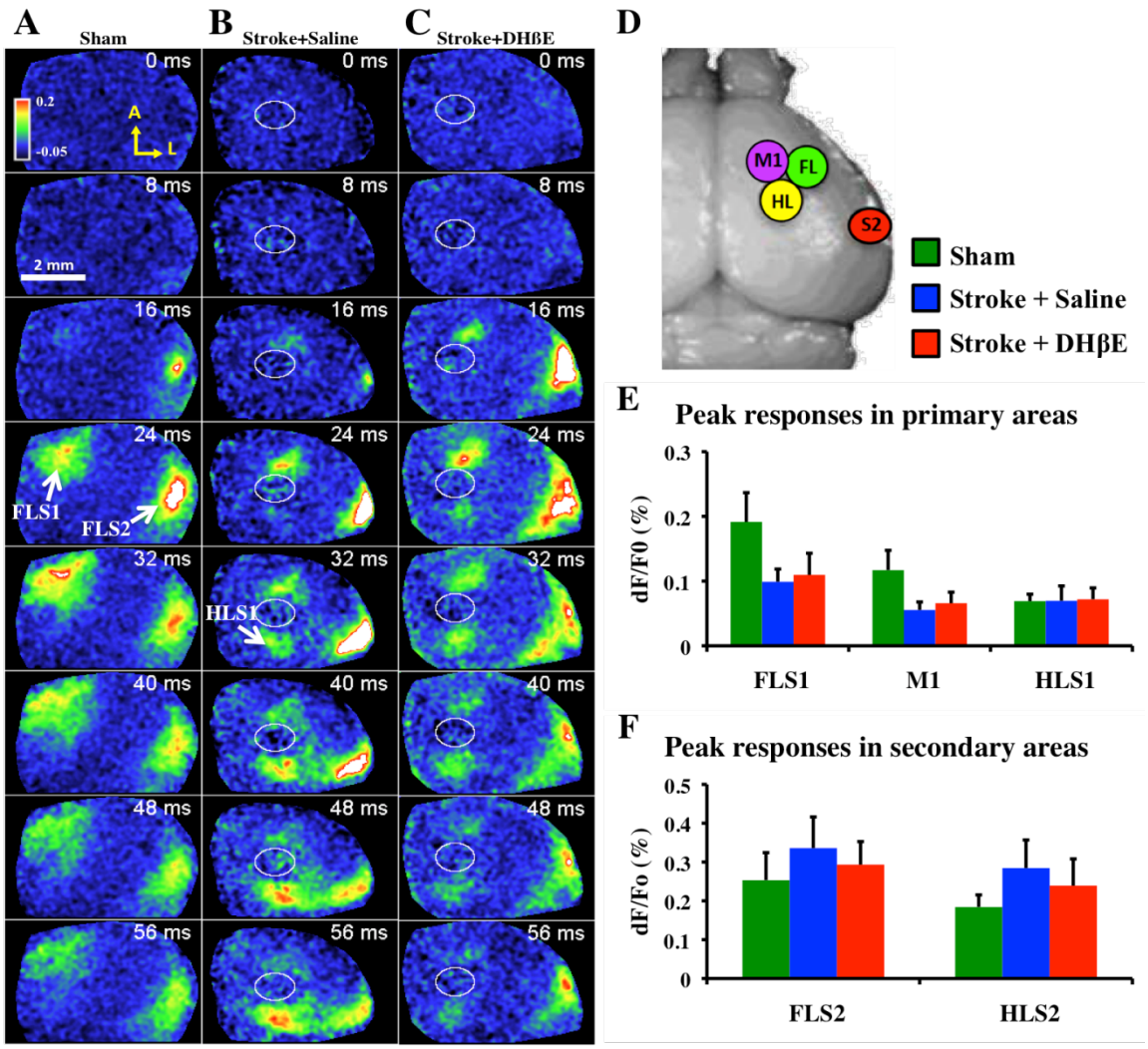

Figure 8. Chronic infusion of DHßE does not affect recovery of cortical responsiveness.

A-C) Representative montages of peak cortical responses following forelimb stimulation in **A)** sham, **B)** stroke + saline, and **C)** stroke + DHßE mice. The white circle indicates the infarct. **D)** Regions from which peak responses were quantified. M1=primary motor area; FL=forelimb primary somatosensory area (FLS1); HL=hindlimb somatosensory area (HLS1); S2=secondary somatosensory area (FLS2 and HLS2). **E-F)** Peak amplitude of cortical responses to forelimb stimulation. **E)** Histogram showing peak responses in primary sensorimotor areas. **F)** Histogram showing peak responses in secondary somatosensory areas. Data are mean ± SEM.

Table 2. Average peak amplitude of forelimb-evoked responses.

	FLS1	M1	HLS1	FLS2	HLS2
Sham	0.19 ± 0.05	0.12 ± 0.03	0.07 ± 0.01	0.25 ± 0.07	0.18 ± 0.03
Stroke+Saline	0.10 ± 0.02	0.06 ± 0.01	0.07 ± 0.02	0.34 ± 0.08	0.28 ± 0.07
Stroke+DHßE	0.11 ± 0.03	0.07 ± 0.02	0.07 ± 0.02	0.29 ± 0.06	0.24 ± 0.07

Average peak cortical responses (peak $\%\Delta F/F_o$) to forelimb stimulation in the forelimb primary somatosensory cortex (FLS1), primary motor cortex (M1), hindlimb primary somatosensory cortex (HLS1), forelimb secondary somatosensory cortex (FLS2), and hindlimb secondary somatosensory cortex (HLS2). Data are mean ± SEM.

Table 3. Average time to peak of forelimb-evoked responses.

	FLS1	M1	HLS1	FLS2	HLS2
Sham	18.40 ± 0.98	25.94 ± 2.33	70.17 ± 23.24	20.46 ± 2.04	63.89 ± 41.62
Stroke+Saline	36.00 ± 10.12	140.80 ± 33.18	129.60 ± 27.48	33.60 ± 11.41	39.20 ± 15.13
Stroke+DHßE	56.67 ± 28.57	144.80 ± 53.30	136.93 ± 52.43	19.07 ± 2.62	25.87 ± 3.21

Average time after forelimb stimulation (ms) of peak cortical responses in each cortical region. Data are mean ± SEM.

Table 4. Average duration of forelimb-evoked responses.

	FLS1	M1	HLS1	FLS2	HLS2
Sham	6.22 ± 0.84	8.93 ± 1.65	14.26 ± 4.15	7.74 ± 1.38	6.98 ± 0.87
Stroke+Saline	6.83 ± 0.95	1.16 ± 0.27	5.74 ± 4.14	7.19 ± 3.58	5.87 ± 2.54
Stroke+DHßE	3.82 ± 1.01	2.91 ± 1.47	4.79 ± 1.52	4.87 ± 0.90	7.51 ± 1.83

Average duration (ms) of cortical responses in each cortical region. Data are mean ± SEM.

sham controls but this effect did not reach significance ($t_{(14)}$=2.10, p=0.06) . There was a significant difference between sham and stroke mice in time to peak ($t_{(10)}$=3.74, p<0.01) and duration ($t_{(10)}$=3.95, p<0.01) of cortical responses in the M1 region (Tables 3-4). These results indicate that chronic DHßE treatment does not significantly alter cortical responses to the affected forepaw.

Chronic α4ß2 nAChR antagonism does not significantly alter infarct volume

Although there were no effects of DHßE on behavioural function or cortical activation, it is possible that DHßE was beneficial if animals in this group suffered larger cerebral infarcts, for reasons unknown or by chance, and still showed the same level of recovery as the saline treated group. To examine this possibility, saline (n=8) and DHßE-treated (n=10) mice were sacrificed 14 weeks after stroke and their brains were sectioned and stained with cresyl violet to measure infarct volume. As expected from behaviour and functional imaging data, long-term α4ß2 nAChR blockade with 1 mg/kg/hr DHßE did not significantly alter infarct volume compared to saline animals. However, there does appear to be a trend towards smaller infarcts in DHßE-treated animals, which agrees with the data from Chapter 2 where DHßE was administered 1.5-3 hours after stroke (Fig. 9; $t_{(10.5)}$=1.36, p=0.20). In summary, this experiment demonstrates that chronic DHßE treatment does not significantly alter the extent of ischemic damage, at least when initiated 24 hours after stroke.

3.4 Discussion

We investigated the effect of chronic treatment with DHßE on long-term stroke recovery using sensorimotor behavioural tests and *in vivo* VSD imaging. Stroke led to an increase in α4ß2 nAChR puncta levels on GABAergic neurons in layer 2/3 of the peri-

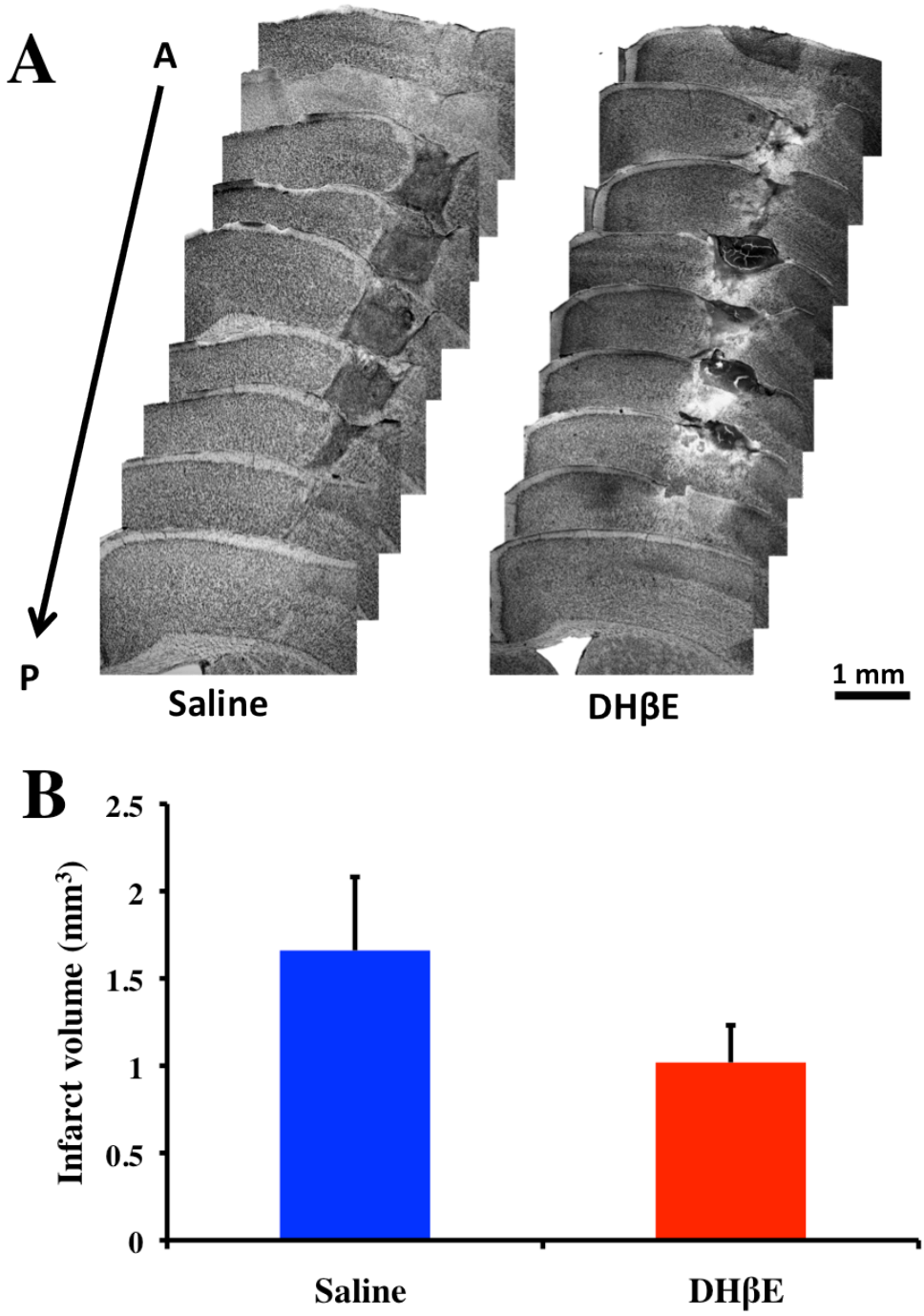

Figure 9. Chronic α4ß2 antagonism does not significantly alter infarct volume.

A) Representative cresyl violet stained coronal sections of the stroke affected hemisphere in mice chronically infused with saline and DHßE. Animals were perfused 14 weeks after stroke. **B)** Histogram showing that DHßE does not significantly alter infarct volume by 14 weeks after stroke. Scale bar=1 mm. Data are mean ± SEM.

infarct cortex one week after stroke. This finding suggested that excessive cortical inhibition after stroke could be mediated by enhanced nicotinic activation of GABAergic neurons. However, contrary to our expectation, chronic α4ß2 nAChR antagonism did not restore sensorimotor function in the forepaw after 10 weeks of recovery, and did not alter cortical responsiveness or infarct volume 14 weeks after stroke. From these data, we can conclude that DHßE does not appear to affect long-term recovery. While there was a specific upregulation of α4ß2 nAChR puncta seen after stroke, the mechanism behind this increase and its implications for stroke rehabilitation remain to be elucidated.

Previous research has demonstrated that α4ß2 nAChRs are upregulated in GABAergic neurons in cortical regions deprived of sensory inputs (Brown et al., 2012). Further, electrophysiological and metabolic imaging studies have shown that cortical activity is reduced in sensory deprived regions (Lendvai et al., 2000; Skibinska et al., 2000). Considering that stroke also leads to a suppression of cortical activity in peri-infarct regions, it is probable that the upregulation of α4ß2 nAChRs 1 week after stroke is a reflection of changes in cortical neuronal activity. At the present time, the functional significance of these changes in α4ß2 nAChR expression is unknown and requires further study.

While there was no effect of DHßE on recovery of forepaw function, our behavioural data is consistent with other studies in demonstrating that the effects of small cortical lesions can be measured over a chronic period when utilizing behavioural measures that are sensitive for the subtle forelimb deficits produced in these lesion models (Schallert, 2006; Shanina et al., 2006; Tennant and Jones, 2009; Sweetnam et al., 2012). We saw that performance on the adhesive tape removal test was restored to baseline levels by 5 to

6 weeks after stroke, and there was very limited recovery on the ladder rung test even at 10 weeks after the stroke, which agrees with previous work from our lab (Sweetnam et al., 2012). Therefore, the absence of an effect of DHßE on functional recovery cannot be attributed to differences in the administration of behavioural testing.

Our data also show that blocking α4ß2 nAChRs does not affect cortical responses to forelimb stimulation as measured by voltage-sensitive dye imaging after 14 weeks of recovery. This result was not unexpected, given that recovery of sensory-motor function is often associated with a return to more normal patterns of brain activity. It is possible that chronic administration of DHßE led to subtle changes in cortical remapping that could have been seen at earlier stages of recovery that may not have been detected at 14 weeks. For instance, previous research has shown that 4 to 7 weeks is a dynamic period when significant improvements are seen in forelimb recovery (Clarkson et al., 2010, 2011; Sweetnam et al., 2012). In our experiments, DHßE treatment ended after 6 weeks of recovery and it may be the case that VSD imaging at this time point would reveal the re-emergence of maps earlier in the treated group, but not in the untreated group. However, since we did not find any behavioural differences between our groups at any time point, this is unlikely. We were able to detect remapping of cortical responses to forelimb stimulation in regions surrounding the infarct at 14 weeks, which is congruous with existing imaging studies and has been reported to occur as early as 8 weeks after stroke (Brown et al., 2009; Sweetnam et al., 2012; Sweetnam and Brown, 2013).

One issue that might be brought to attention is that strokes were performed in anaesthetized mice even though we have presented data in Chapter 2 showing that isoflurane masks the effect of DHBE in neuroprotection. Firstly, the experiments

performed in Chapter 3 were designed to explore the role of α4ß2 nAChRs in chronic stroke recovery. Chronic DHßE treatment began at a time point (24 hours) after which most of the infarct core is established (Saver, 2006). Moreover, the mechanisms underlying neuroprotection from necrotic and apoptotic cell death are not the same as those involved in enhancing long-term plasticity and functional recovery. Additionally, studies in humans have shown that lesion size is a poor predictor of functional recovery (Chen et al., 2000; Page et al., 2013). Therefore it is reasonable to presume that the neuroprotective effect of isoflurane on lesion size would not have significant interactions with any effect of DHßE administration on chronic recovery in our experimental design.

While the outcomes of this study were unremarkable, there are several issues that may have contributed to these results. First, the dose of DHßE used for chronic treatment was based on a previous study that examined nicotinic involvement in experience based cortical plasticity in healthy mice (Brown et al., 2012). Ischemia may amplify nAChR signalling, as evidenced by the increased expression level of α4-YFP puncta, to a degree that requires a higher dose in order to yield a therapeutic outcome. Future research will need to investigate whether or not higher doses or direct infusion of DHßE into the brain can be beneficial for long-term recovery. On that note, the relationship between α4ß2 nAChRs and GABAergic signalling described in studies of experience-dependent cortical plasticity and chronic nicotine administration were also observed in normal, healthy subjects (Nashmi et al., 2007; Brown et al., 2012). The consequences of ischemia are chaotic at the cellular level, and involve many other events besides α4ß2 nAChR upregulation. The interaction between increased cholinergic signalling and other processes including electrical dysfunction, inflammation, ROS production and apoptosis

may result in a completely different outcome in the ischemic brain than what is seen in healthy subjects. Furthermore, the expression of α4ß2 nAChRs in the brain is widespread and these receptors have been identified on many different types of cells. Although we saw changes in puncta expression on GABAergic cells, we did not quantify changes in α4-YFP puncta on other types of neurons. It is possible that the increase in α4ß2 nAChRs also occurred on excitatory pyramidal cells, in which case α4ß2 nAChR antagonism would confer a different consequence, possibly further enhancing cortical inhibition. It will be important to characterize other cell types that are affected by changes in cholinergic signalling to identify other mechanisms by which α4ß2 nAChRs are involved in functional recovery. Finally, to determine if α4ß2 nAChRs truly play a role in excessive inhibition during stroke recovery, it would be important to perform electrophysiological experiments to determine the effect of DHßE treatment on GABAergic excitability in ischemic tissue. In conclusion, the long-term effects of increased expression of α4ß2 nicotinic acetylcholine receptors after ischemia and its therapeutic implications, if any, are still unknown given that chronic nAChR antagonism does not lead to significant improvements in functional outcome or cortical excitability.

Chapter 4: General Conclusions

The main objective of this study was to characterize the role of α4ß2 nicotinic acetylcholine receptors on neuroprotection and recovery from ischemic stroke. In our neuroprotection experiments, we induced a targeted photothrombotic stroke in the middle cerebral artery in mice that were given acute treatment after ischemia with vehicle or the α4ß2 nAChR-specific antagonist DHßE in awake and anaesthetized conditions. In the chronic recovery experiments, we induced a photothrombotic stroke in the forelimb somatosensory cortex to assess the behavioural performance and cortical responsiveness in mice chronically treated with vehicle or DHßE. From these studies, we report three major findings:

1. Treatment with 3 mg/kg of DHßE acutely after stroke triggered neuroprotection and reduced lesion size 1 day after stroke. The effect was not a consequence of increased collateral flow to the penumbral tissue.
2. The expression of α4ß2 nAChR puncta was upregulated in the peri-infarct cortex. Increased expression was found on GABAergic neurons in the peri-infarct tissue relative to the contralesional homotopic cortex. However, chronic antagonism of α4ß2 nAChRs with 1 mg/kg/hr DHßE did not enhance recovery of forelimb function, increase cortical responsiveness or reduce infarct volume at 14 weeks after stroke.
3. The use of isoflurane in a well-established stroke model can conceal the effect of drug treatments on neuroprotection.

These findings suggest that ischemic stroke causes changes in nAChRs. Suppressing the activation of these receptors acutely promotes neuroprotection, but blocking α4ß2 nAChRs chronically does not enhance long-term functional recovery.

In addition, we showed that administration of an anaesthetic is a confound in neuroprotection studies. This finding has critical implications for the field of stroke research. Considering the vast number of drugs that have failed when transitioned from the basic science laboratory into clinical trials, it is likely that our current stroke models lead us to miss potential therapies. In view of the fact that the occurrence of stroke in the human population does not happen under anaesthesia, we have developed a novel protocol of inducing photothrombotic stroke in freely moving animals that may lead to greater transition of therapeutics from bench to bedside.

Overall, our findings provide evidence that cholinergic signalling is altered in stroke pathophysiology. Research on the role of α4ß2 nicotinic receptors in ischemic stroke is nascent and full of potential. Their extensive participation in neurotransmitter signalling, among other properties, makes α4ß2 nicotinic acetylcholine receptors a likely candidate for mediating cellular and synaptic health and plasticity in stroke. Future exploration of this novel mechanism will provide a new understanding of the processes underlying acute and long-term changes in brain function following ischemic stroke.

Bibliography

Abbruscato TJ, Lopez SP, Mark KS, Hawkins BT, Davis TP (2002) Nicotine and cotinine modulate cerebral microvascular permeability and protein expression of ZO-1 through nicotinic acetylcholine receptors expressed on brain endothelial cells. Journal of Pharmaceutical Sciences 91:2525–2538.

Adibhatla RM, Hatcher JF (2003) Citicoline decreases phospholipase A2 stimulation and hydroxyl radical generation in transient cerebral ischemia. Journal of Neuroscience Research 73:308–315.

Akaike A, Tamura Y, Yokota T, Shimohama S, Kimura J (1994) Nicotine-induced protection of cultured cortical neurons against N-methyl-D-aspartate receptor-mediated glutamate cytotoxicity. Brain Research 644:181–187.

Akpan N, Troy CM (2012) Caspase Inhibitors: Prospective Therapies for Stroke. The Neuroscientist:1–8.

Alkondon M, Pereira EF, Eisenberg HM, Albuquerque EX (2000) Nicotinic receptor activation in human cerebral cortical interneurons: a mechanism for inhibition and disinhibition of neuronal networks. Journal of Neuroscience 20:66–75.

Alkondon M, Periera EFR, Albuquerque EX (1996) Mapping the Location of Functional Nicotinic and gamma-Aminobutyric Acid(A) Receptors on Hippocampal Neurons. Journal of Pharmacology and Experimental Therapeutics 279:1491–1506.

Anand R, Conroy WG, Schoepfer R, Whiting P, Lindstrom J (1991) Neuronal nicotinic acetylcholine receptors expressed in Xenopus oocytes have a pentameric quaternary structure. Journal of Biological Chemistry 266:11192–11198.

Public Health Agency of Canada (2009) Tracking Heart Disease and Stroke in Canada.

Armitage GA, Todd KG, Shuaib A, Winship IR (2010) Laser speckle contrast imaging of collateral blood flow during acute ischemic stroke. Journal of Cerebral Blood Flow and Metabolism 30:1432–1436.

Atochin DN, Wang A, Liu VWT, Critchlow JD, Dantas AP V, Looft-wilson R, Murata T, Salomone S, Shin HK, Ayata C, Moskowitz MA, Michel T, Sessa WC, Huang PL (2007) The phosphorylation state of eNOS modulates vascular reactivity and outcome of cerebral ischemia in vivo. Journal of Clinical Investigation 117:1961–1967.

Bang OY, Saver JL, Buck BH, Alger JR, Starkman S, Ovbiagele B, Kim D, Jahan R, Duckwiler GR, Yoon SR, Vinuela F, Liebeskind DS (2009) Impact of collateral flow on tissue fate in acute ischaemic stroke. Journal of Neurology, Neurosurgery & Psychiatry 79:625–629.

Beck J, Lenart B, Kintner DB, Sun D (2003) Na-K-Cl cotransporter contributes to glutamate-mediated excitotoxicity. Journal of Neuroscience 23:5061–5068.

Benveniste H, Drejer J, Schousboe A, Diemer NH (1984) Elevation of the extracellular concentrations of glutamate and aspartate in rat hippocampus during transient cerebral ischemia monitored by intracerebral microdialysis. Journal of Neurochemistry 43:1369–1374.

Bleilevens C, Roehl AB, Goetzenich A, Zoremba N, Kipp M, Dang J, Tolba R, Rossaint R, Hein M (2012) Effect of anesthesia and cerebral blood flow on neuronal injury in a rat middle cerebral artery occlusion (MCAO) model. Experimental Brain Research.

Boden-Albala B, Sacco RL, Lee H-S, Grahame-Clarke C, Rundek T, Elkind M V, Wright C, Giardina E-G V, DiTullio MR, Homma S, Paik MC (2008) Metabolic syndrome and ischemic stroke risk: Northern Manhattan Study. Stroke 39:30–35.

Brannigan G, Lebard DN, Hénin J, Eckenhoff RG, Klein ML (2010) Multiple binding sites for the general anesthetic isoflurane identified in the nicotinic acetylcholine receptor transmembrane domain. PNAS 207:14122–14127.

Broughton BRS, Reutens DC, Sobey CG (2009) Apoptotic mechanisms after cerebral ischemia. Stroke 40:e331–9.

Brown CE, Aminoltejari K, Erb H, Winship IR, Murphy TH (2009) In vivo voltage-sensitive dye imaging in adult mice reveals that somatosensory maps lost to stroke are replaced over weeks by new structural and functional circuits with prolonged modes of activation within both the peri-infarct zone and distant sites. Journal of Neuroscience 29:1719–1734.

Brown CE, Boyd JD, Murphy TH (2010) Longitudinal in vivo imaging reveals balanced and branch-specific remodeling of mature cortical pyramidal dendritic arbors after stroke. Journal of Cerebral Blood Flow and Metabolism 30:783–791.

Brown CE, Li P, Boyd JD, Delaney KR, Murphy TH (2007) Extensive turnover of dendritic spines and vascular remodeling in cortical tissues recovering from stroke. Journal of Neuroscience 27:4101–4109.

Brown CE, Sweetnam D, Beange M, Nahirney PC, Nashmi R (2012) α4* Nicotinic acetylcholine receptors modulate experience-based cortical depression in the adult mouse somatosensory cortex. Journal of Neuroscience 32:1207–1219.

Brown DA (2010) Muscarinic acetylcholine receptors (mAChRs) in the nervous system: some functions and mechanisms. Journal of Molecular Neuroscience 41:340–346.

Buckingham SD, Jones AK, Brown LA, Sattelle DB (2009) Nicotinic Acetylcholine Receptor Signalling: Roles in Alzheimer's Disease and Amyloid Neuroprotection. Pharmacological Reviews 61:39–61.

Busch E, Gyngell ML, Eis M, Hoehn-Berlage M, Hossmann KA (1996) Potassium-induced cortical spreading depressions during focal cerebral ischemia in rats: contribution to lesion growth assessed by diffusion-weighted NMR and biochemical imaging. Journal of Cerebral Blood Flow and Metabolism 16:1090–1099.

Carmichael ST (2005) Rodent models of focal stroke: size, mechanism, and purpose. Experimental Neurotherapeutics 2:396–409.

Carmichael ST, Archibeque I, Luke L, Nolan T, Momiy J, Li S (2005) Growth-associated gene expression after stroke: evidence for a growth-promoting region in peri-infarct cortex. Experimental Neurology 193:291–311.

Carmichael ST, Wei L, Rovainen CM, Woolsey T a (2001) New patterns of intracortical projections after focal cortical stroke. Neurobiology of Disease 8:910–922.

Chen CL, Tang FT, Chen HC, Chung CY, Wong MK (2000) Brain lesion size and location: effects on motor recovery and functional outcome in stroke patients. Archives of Physical Medicine and Rehabilitation 81:447–452.

Clark WM, Wissman S, Albers GW, Jhamandas JH, Hamilton S (1999) Recombinant Tissue-Type Plasminogen Activator (Alteplase) for Ischemic Stroke 3 to 5 Hours After Symptom Onset. Journal of the American Medical Association 282:2019–2026.

Clarkson AN, Huang BS, MacIsaac SE, Mody I, Carmichael ST (2010) Reducing excessive GABA-mediated tonic inhibition promotes functional recovery after stroke. Nature 468:305–309.

Clarkson AN, Overman JJ, Zhong S, Mueller R, Lynch G, Carmichael ST (2011) AMPA receptor-induced local brain-derived neurotrophic factor signaling mediates motor recovery after stroke. Journal of Neuroscience 31:3766–3775.

Dancause N, Barbay S, Frost SB, Plautz EJ, Chen D, Zoubina E V, Stowe AM, Nudo RJ (2005) Extensive cortical rewiring after brain injury. Journal of Neuroscience 25:10167–10179.

Dickinson R, Peterson BK, Banks P, Simillis C, Martin JCS, Valenzuela CA, Maze M, Franks NP (2007) Competitive Inhibition at the Glycine Site of the N-Methyl- D - aspartate Receptor by the Anesthetics Xenon and Isoflurane. Anesthesiology 107:756–767.

Dijkhuizen RM, Ren J, Mandeville JB, Wu O, Ozdag FM, Moskowitz MA, Rosen BR, Finklestein SP (2001) Functional magnetic resonance imaging of reorganization in rat brain after stroke. PNAS 98:12766–12771.

Dijkhuizen RM, Singhal AB, Mandeville JB, Wu O, Halpern EF, Finklestein SP, Rosen BR, Lo EH (2003) Correlation between brain reorganization, ischemic damage, and neurologic status after transient focal cerebral ischemia in rats: a functional magnetic resonance imaging study. Journal of Neuroscience 23:510–517.

Dirnagl U, Iadecola C, Moskowitz MA (1999) Pathobiology of ischaemic stroke: an integrated view. Trends in Neurosciences 22:391–397.

Domann R, Hagemann G, Kraemer M, Freund HJ, Witte OW (1993) Electrophysiological changes in the surrounding brain tissue of photochemically induced cortical infarcts in the rat. Neuroscience Letters 155:69–72.

Domino EF, Minoshima S, Guthrie SK, Ohl L, Ni L, Koeppe RA, Cross DJ, Zubieta J-K (2000) Effects of nicotine on regional cerebral glucose metabolism in awake resting tobacco smokers. Neuroscience 101:277–282.

Farrant M, Nusser Z (2005) Variations on an inhibitory theme: phasic and tonic activation of GABA(A) receptors. Nature Reviews Neuroscience 6:215–229.

Feng G, Mellor RH, Bernstein M, Keller-Peck C, Nguyen QT, Wallace M, Nerbonne JM, Lichtman JW, Sanes JR (2000) Imaging neuronal subsets in transgenic mice expressing multiple spectral variants of GFP. Neuron 28:41–51.

Fenster CP, Rains MF, Noerager B, Quick MW, Lester RA (1997) Influence of subunit composition on desensitization of neuronal acetylcholine receptors at low concentrations of nicotine. Journal of Neuroscience 17:5747–5759.

Fink K, Zhu J, Namura S, Shimizu-Sasamata M, Endres M, Ma J, Dalkara T, Yuan J, Moskowitz M a (1998) Prolonged therapeutic window for ischemic brain damage caused by delayed caspase activation. Journal of Cerebral Blood Flow and Metabolism 18:1071–1076.

Flood P, Ramirez-Latorre J, Role L (1997) α4β2 neuronal nicotinic acetylcholine receptors in the central nervous system are inhibited by isoflurane and propofol, but a7-type nicotinic acetylcholine receptors are unaffected. Anesthesiology 86:859–865.

Friberg H, Ferrand-Drake M, Bengtsson F, Halestrap a P, Wieloch T (1998) Cyclosporin A, but not FK 506, protects mitochondria and neurons against hypoglycemic damage and implicates the mitochondrial permeability transition in cell death. Journal of Neuroscience 18:5151–5159.

Furukawa S, Sameshima H, Yang L, Ikenoue T (2012) Activation of acetylcholine receptors and microglia in hypoxic-ischemic brain damage in newborn rats. Brain & Development.

Galzi J, Changeux J (1995) Neuronal Nicotinic Receptors : Molecular Organization and Regulations. Neuropharmacology 34:563–582.

Gemba T, Oshima T, Ninomiya M (1994) Glutamate efflux via the reversal of the sodium-dependent glutamate transporter caused by glycolytic inhibition in rat cultured astrocytes. Neuroscience 63:789–795.

Go AS et al. (2013) Heart Disease and Stroke Statistics--2013 Update: A Report From the American Heart Association. Circulation 127:e6–e245.

Gorter JA, Petrozzino JJ, Aronica EM, Rosenbaum DM, Opitz T, Bennett M V, Connor JA, Zukin RS (1997) Global ischemia induces downregulation of Glur2 mRNA and increases AMPA receptor-mediated Ca2+ influx in hippocampal CA1 neurons of gerbil. Journal of Neuroscience 17:6179–6188.

Graham SH (2011) Inflammation After Stroke: Mechanisms and Therapeutic Approaches. Translational Stroke Research 1:74–84.

Granon S, Poucet B, Thinus-Blanc C, Changeux JP, Vidal C (1995) Nicotinic and muscarinic receptors in the rat prefrontal cortex: differential roles in working memory, response selection and effortful processing. Psychopharmacology 119:139–144.

The National Institute of Neurological Disorders and Stroke rt-PA Stroke Study Group (NINDS) (1995) Tissue plasminogen activator for acute ischemic stroke. New England Journal of Medicine 333:1581–1587.

Guan Z-Z, Yu W-F, Nordberg A (2003) Dual effects of nicotine on oxidative stress and neuroprotection in PC12 cells. Neurochemistry International 43:243–249.

Hagemann G, Redecker C, Neumann-Haefelin T, Freund HJ, Witte OW (1998) Increased long-term potentiation in the surround of experimentally induced focal cortical infarction. Annals of Neurology 44:255–258.

Hansen AJ, Zeuthen T (1981) Extracellular ion concentrations during spreading depression and ischemia in the rat brain cortex. Acta Physiologica Scandinavica 113:437–445.

Harris RJ, Symon L, Branston NM, Bayhan M (1981) Changes in extracellular calcium activity in cerebral ischaemia. Journal of Cerebral Blood Flow and Metabolism 1:203–209.

Hawkins BT, Abbruscato TJ, Egleton RD, Brown RC, Huber JD, Campos CR, Davis TP (2004) Nicotine increases in vivo blood-brain barrier permeability and alters cerebral microvascular tight junction protein distribution. Brain Research 1027:48–58.

Hawkins BT, Brown RC, Davis TP (2002) Smoking and ischemic stroke: a role for nicotine? Trends in Pharmacological Sciences 23:78–82.

Hawkins BT, Egleton RD, Davis TP (2005) Modulation of cerebral microvascular permeability by endothelial nicotinic acetylcholine receptors. American Journal of Physiology: Heart and Circulatory Physiology 289:H212–9.

Herrmann KS (1983) Platelet Aggregation Photochemical Induced in the Hamster Cheek Pouch by a Process with Excited Fluorescein Isothiacyanate-Dextran. Microvascular Research 249:238–249.

Hill JW, Poddar R, Thompson JF, Rosenberg G a, Yang Y (2012) Intranuclear matrix metalloproteinases promote DNA damage and apoptosis induced by oxygen-glucose deprivation in neurons. Neuroscience 220:277–290.

Hoang MV, Nagy JA, Fox JEB, Senger DR (2010) Moderation of calpain activity promotes neovascular integration and lumen formation during VEGF-induced pathological angiogenesis. PLOS One 5:e13612.

Hong SC, Lanzino G, Goto Y, Kang SK, Schottler F, Kassell NF, Lee KS (1994) Calcium-activated proteolysis in rat neocortex induced by transient focal ischemia. Brain Research 661:43–50.

Hossmann KA (1994) Viability thresholds and the penumbra of focal ischemia. Annals of Neurology 36:557–565.

Hosur V, Loring RH (2011) α4ß2 Nicotinic Receptors Partially Mediate Anti-Inflammatory Effects through Janus Kinase 2-Signal Transducer and Activator of Transcription 3 but Not Calcium or cAMP Singaling. Molecular Pharmacology 79:167–174.

Hu X, Zhang Y, Zeng F (2004) Effects of sodium beta-aescin on expression of adhesion molecules and migration of neutrophils after middle cerebral artery occlusion in rats. Acta Pharmacologica Sinica 25:869–875.

Iadecola C, Anrather J (2011) The immunology of stroke: from mechanisms to translation. Nature Medicine 17:796–808.

Jones IW, Bolam JP, Wonnacott S (2001) Presynaptic localisation of the nicotinic acetylcholine receptor beta2 subunit immunoreactivity in rat nigrostriatal dopaminergic neurones. The Journal of Comparative Neurology 439:235–247.

Jones IW, Wonnacott S (2004) Precise localization of alpha7 nicotinic acetylcholine receptors on glutamatergic axon terminals in the rat ventral tegmental area. Journal of Neuroscience 24:11244–11252.

Kapinya KJ, Prass K, Dirnagl U (2002) Isoflurane induced prolonged protection against cerebral ischemia in mice: a redox sensitive mechanism? Neuroreport 13:1431–1435.

Kenny PJ, File SE, Neal MJ (2000) Evidence for a complex influence of nicotinic acetylcholine receptors on hippocampal serotonin release. Journal of Neurochemistry 75:2409–2414.

Ketheeswaranathan P, Turner NA, Spary EJ, Batten TFC, McColl BW, Saha S (2011) Changes in glutamate transporter expression in mouse forebrain areas following focal ischemia. Brain Research 1418:93–103.

Khatibi NH, Ma Q, Rolland W, Ostrowski R, Fathali N, Martin R, Applegate R, Stier G, Tang J, Zhang JH (2011) Isoflurane posttreatment reduces brain injury after an intracerebral hemorrhagic stroke in mice. Anesthesia and Analgesia 113:343–348.

Kissela BM, Khoury J, Kleindorfer D, Woo D, Schneider A, Alwell K, Miller R, Ewing I, Moomaw CJ, Szaflarski JP, Gebel J, Shukla R, Broderick JP (2005) Epidemiology of Ischemic Stroke in Patients with Diabetes. Diabetes Care 28:355–359.

Kristian T, Siesjo BK (1998) Calcium in Ischemic Cell Death. Stroke 29:705–718.

Kunz A, Dirnagl U, Mergenthaler P (2010) Acute pathophysiological processes after ischaemic and traumatic brain injury. Best Practice & Research Clinical Anaesthesiology 24:495–509.

Lakhan SE, Kirchgessner A, Hofer M (2009) Inflammatory mechanisms in ischemic stroke: therapeutic approaches. Journal of Translational Medicine 7:97.

Lambe EK, Picciotto MR, Aghajanian GK (2003) Nicotine induces glutamate release from thalamocortical terminals in prefrontal cortex. Neuropsychopharmacology 28:216–225.

Le DA, Wu Y, Huang Z, Matsushita K, Plesnila N, Augustinack JC, Hyman BT, Yuan J, Kuida K, Flavell RA, Moskowitz MA (2002) Caspase activation and neuroprotection in caspase-3- deficient mice after in vivo cerebral ischemia and in vitro oxygen glucose deprivation. PNAS 99:15188–15193.

Lendvai B, Stern E a, Chen B, Svoboda K (2000) Experience-dependent plasticity of dendritic spines in the developing rat barrel cortex in vivo. Nature 404:876–881.

Li Y, Xiao D, Dasgupta C, Xiong F, Tong W, Yang S, Zhang L (2012) Perinatal nicotine exposure increases vulnerability of hypoxic-ischemic brain injury in neonatal rats: role of angiotensin II receptors. Stroke 43:2483–2490.

Liebeskind DS (2003) Collateral circulation. Stroke 34:2279–2284.

Lloyd-Jones D et al. (2010) Heart disease and stroke statistics--2010 update: a report from the American Heart Association. Circulation 121:e46–e215.

Lozano R et al. (2012) Global and regional mortality from 235 causes of death for 20 age groups in 1990 and 2010: a systematic analysis for the Global Burden of Disease Study 2010. The Lancet 380:2095–2128.

Metherate R (2004) Nicotinic acetylcholine receptors in sensory cortex. Learning & Memory 11:50–59.

Metz GA, Whishaw IQ (2002) Cortical and subcortical lesions impair skilled walking in the ladder rung walking test: a new task to evaluate fore- and hindlimb stepping, placing, and co-ordination. Journal of Neuroscience Methods 115:169–179.

Millar NS, Gotti C (2009) Diversity of vertebrate nicotinic acetylcholine receptors. Neuropharmacology 56:237–246.

Miwa JM, Freedman R, Lester HA (2011) Neural systems governed by nicotinic acetylcholine receptors: emerging hypotheses. Neuron 70:20–33.

Moody EJ, Harris BD, Skolnick P (1993) Stereospecific actions of the inhalation anesthetic isoflurane at the GABAA receptor complex. Brain Research 615:101–106.

Mori E, Del Zoppo GJ, Chambers JD, Copeland BR, Arfors KE (1992) Inhibition of polymorphonuclear leukocyte adherence suppresses no-reflow after focal cerebral ischemia in baboons. Stroke 23:712–718.

Moskowitz MA, Lo EH, Iadecola C (2010) The science of stroke: Mechanisms in search of treatments. Neuron 67:181–198.

Murphy TH, Corbett D (2009) Plasticity during stroke recovery: From synapse to behaviour. Nature Reviews Neuroscience 10:861–872.

Murphy TH, Li P, Betts K, Liu R (2008) Two-photon imaging of stroke onset in vivo reveals that NMDA-receptor independent ischemic depolarization is the major cause of rapid reversible damage to dendrites and spines. Journal of Neuroscience 28:1756–1772.

Murphy TH, Malouf AT, Sastre A, Schnaar RL, Coyle JT (1988) Calcium-dependent glutamate cytotoxicity in a neuronal cell line. Brain Research 444:325–332.

Nakamura M, Jang I-S (2010) Presynaptic nicotinic acetylcholine receptors enhance GABAergic synaptic transmission in rat periaqueductal gray neurons. European Journal of Pharmacology 640:178–184.

Namura S, Zhu J, Fink K, Endres M, Srinivasan A, Tomaselli KJ, Yuan J, Moskowitz M a (1998) Activation and cleavage of caspase-3 in apoptosis induced by experimental cerebral ischemia. Journal of Neuroscience 18:3659–3668.

Nanetti L, Raffaelli F, Vignini A, Perozzi C, Silvestrini M, Bartolini M, Provinciali L, Mazzanti L (2011) Oxidative stress in ischaemic stroke. European Journal of Clinical Investigation 41:1318–1322.

Nashmi R, Lester HA (2006) CNS Localization of Neuronal Nicotinic Receptors. Journal of Molecular Neuroscience 30:181–184.

Nashmi R, Xiao C, Deshpande P, McKinney S, Grady SR, Whiteaker P, Huang Q, McClure-Begley T, Lindstrom JM, Labarca C, Collins AC, Marks MJ, Lester HA (2007) Chronic nicotine cell specifically upregulates functional alpha 4* nicotinic receptors: basis for both tolerance in midbrain and enhanced long-term potentiation in perforant path. Journal of Neuroscience 27:8202–8218.

Nedergaard M, Astrup J (1986) Infarct rim: effect of hyperglycemia on direct current potential and [14C]2-deoxyglucose phosphorylation. Journal of Cerebral Blood Flow and Metabolism 6:607–615.

Nelson ME, Kuryatov A, Choi CH, Zhou Y, Lindstrom J (2003) Alternate stoichiometries of alpha4beta2 nicotinic acetylcholine receptors. Molecular Pharmacology 63:332–341.

Neumann J, Gunzer M, Gutzeit HO, Ullrich O, Reymann KG, Dinkel K (2006) Microglia provide neuroprotection after ischemia. FASEB 20:714–716.

Neumann-Haefelin T, Hagemann G, Witte OW (1995) Cellular correlates of neuronal hyperexcitability in the vicinity of photochemically induced cortical infarcts in rats in vitro. Neuroscience Letters 193:101–104.

Nogueira RG, Smith WS, Sung G, Duckwiler G, Walker G, Roberts R, Saver JL, Liebeskind DS (2011) Effect of time to reperfusion on clinical outcome of anterior circulation strokes treated with thrombectomy: pooled analysis of the MERCI and Multi MERCI trials. Stroke 42:3144–3149.

Page SJ, Gauthier L V, White S (2013) Size Doesn't Matter: Cortical Stroke Lesion Volume Is Not Associated With Upper Extremity Motor Impairment and Function in Mild, Chronic Hemiparesis. Archives of Physical Medicine and Rehabilitation 1.

Paterson D, Nordberg A (2000) Neuronal nicotinic receptors in the human brain. Progress in Neurobiology 61:75–111.

Peixoto PM, Lue JK, Ryu S-Y, Wroble BN, Sible JC, Kinnally KW (2011) Mitochondrial apoptosis-induced channel (MAC) function triggers a Bax/Bak-dependent bystander effect. The American Journal of Pathology 178:48–54.

Pettegrew JW, Panchalingam K, Mcclure RJ, Levine J (2001) Brain Metabolic Effects of Acute Nicotine. Neurochemical Research 26:181–185.

Piantadosi CA, Zhang J (1996) Mitochondrial Generation of Reactive Oxygen Species After Brain Ischemia in the Rat. Stroke 27 :327–332.

Pimlott SL, Piggott M, Owens J, Greally E, Court J a, Jaros E, Perry RH, Perry EK, Wyper D (2004) Nicotinic acetylcholine receptor distribution in Alzheimer's disease, dementia with Lewy bodies, Parkinson's disease, and vascular dementia: in vitro binding study using 5-[(125)i]-a-85380. Neuropsychopharmacology 29:108–116.

Rada EM, Tharakan EC, Flood P (2003) Volatile Anesthetics Reduce Agonist Affinity at Nicotinic Acetylcholine Receptors in the Brain. Anesthetic Pharmacology 96:108–111.

Radius RL, Anderson DR (1980) Distribution of albumin in the normal monkey eye as revealed by Evans blue fluorescence microscopy. Investigative Ophthalmology & Visual Science 19:238–243.

Rami A, Sims J, Botez G, Winckler J (2003) Spatial resolution of phospholipid scramblase 1 (PLSCR1), caspase-3 activation and DNA-fragmentation in the human hippocampus after cerebral ischemia. Neurochemistry International 43:79–87.

Redecker C, Wang W, Fritschy J, Witte OW (2002) Widespread and Long-Lasting Alterations in GABA A -Receptor Subtypes After Focal Cortical Infarcts in Rats: Mediation by NMDA-Dependent Processes. Journal of Cerebral Blood Flow and Metabolism 22:1463–1475.

Risher WC, Ard D, Yuan J, Kirov S a (2010) Recurrent spontaneous spreading depolarizations facilitate acute dendritic injury in the ischemic penumbra. Journal of Neuroscience 30:9859–9868.

Romanic AM, White RF, Arleth AJ, Ohlstein EH, Barone FC, Dawson VL (1998) Matrix Metalloproteinase Expression Increases After Cerebral Focal Ischemia in Rats: Inhibition of Matrix Metalloproteinase-9 Reduces Infarct Size. Stroke 29:1020–1030.

Sahlas DJ, Gould L, Swartz RH, Mohammed N, McNicoll-Whiteman R, Naufal F, Oczkowski W (2013) Tissue Plasminogen Activator Overdose in Acute Ischemic Stroke Patients Linked to Poorer Functional Outcomes. Journal of Stroke and Cerebrovascular Diseases:1–5.

Sargent PB (1993) The diversity of neuronal nicotinic acetylcholine receptors. Annual Review of Neuroscience 16:403–443.

Saver JL (2006) Time is brain--quantified. Stroke 37:263–266.

Schallert T (2006) Behavioral tests for preclinical intervention assessment. Experimental Neurotherapeutics 3:497–504.

Schiene K, Bruehl C, Zilles K, Qü M, Hagemann G, Kraemer M, Witte OW (1996) Neuronal hyperexcitability and reduction of GABAA-receptor expression in the surround of cerebral photothrombosis. Journal of Cerebral Blood Flow and Metabolism 16:906–914.

Schwinn DA, McIntyre RW, Reves JG (1990) Isoflurane-induced vasodilation: role of the alpha-adrenergic nervous system. Anesthesia and Analgesia 71:451–459.

Séguéla P, Wadiche J, Dineley-Miller K, Dani J a, Patrick JW (1993) Molecular cloning, functional properties, and distribution of rat brain alpha 7: a nicotinic cation channel highly permeable to calcium. Journal of Neuroscience 13:596–604.

Shameem M, Patel AB (2012) Glutamatergic and GABAergic metabolism in mouse brain under chronic nicotine exposure: implications for addiction. PLOS One 7:e41824.

Shanina EV, Schallert T, Witte OW, Redecker C (2006) Behavioral recovery from unilateral photothrombotic infarcts of the forelimb sensorimotor cortex in rats: Role of the contralateral cortex. Neuroscience 139:1495–1506.

Sheardown MJ (1997) The triggering of spreading depression in the chick retina by nicotinic receptor agonists. European Journal of Pharmacology 337:209–212.

Sieber MW, Jaenisch N, Brehm M, Guenther M, Linnartz-Gerlach B, Neumann H, Witte OW, Frahm C (2013) Attenuated inflammatory response in triggering receptor expressed on myeloid cells 2 (TREM2) knock-out mice following stroke. PLOS One 8:e52982.

Siemkowicz E, Hansen AJ (1981) Brain extracellular ion composition and EEG activity following 10 minutes ischemia in normo- and hyperglycemic rats. Stroke 12:236–240.

Skibinska A, Glazewski S, Fox K, Kossut M (2000) Age-dependent response of the mouse barrel cortex to sensory deprivation : a 2-deoxyglucose study. Experimental Brain Research 132:134–138.

Stanika RI, Villanueva I, Kazanina G, Andrews SB, Pivovarova NB (2012) Comparative impact of voltage-gated calcium channels and NMDA receptors on mitochondria-mediated neuronal injury. Journal of Neuroscience 32:6642–6650.

Stevens TR, Krueger SR, Fitzsimonds RM, Picciotto MR (2003) Neuroprotection by nicotine in mouse primary cortical cultures involves activation of calcineurin and L-type calcium channel inactivation. Journal of Neuroscience 23:10093–10099.

Stroemer RP, Kent TA, Hulsebosch CE (1995) Neocortical Neural Sprouting, Synaptogenesis, and Behavioral Recovery After Neocortical Infarction in Rats. Stroke 26 :2135–2144.

Sugawara T, Fujimura M, Noshita N, Kim GW, Saito A, Hayashi T, Narasimhan P, Maier CM, Chan PH (2004) Neuronal death/survival signaling pathways in cerebral ischemia. Experimental Neurotherapeutics 1:17–25.

Sweetnam D, Holmes A, Tennant KA., Zamani A, Walle M, Jones P, Wong C, Brown CE (2012) Diabetes Impairs Cortical Plasticity and Functional Recovery Following Ischemic Stroke. Journal of Neuroscience 32:5132–5143.

Sweetnam DA, Brown CE (2013) Stroke induces long-lasting deficits in the temporal fidelity of sensory processing in the somatosensory cortex. Journal of Cerebral Blood Flow and Metabolism 33:91–96.

Takada Y, Yonezawa A, Kume T, Katsuki H, Kaneko S, Sugimoto H, T DPY, Neuropharmacology SK (2003) Nicotinic Acetylcholine Receptor-Mediated Neuroprotection by Donepezil Against Glutamate Neurotoxicity in Rat Cortical Neurons. Journal of Pharmacology and Experimental Therapeutics 306:772–777.

Tansey EM (2006) Henry Dale and the discovery of acetylcholine. Comptes Rendus Biologies 329:419–425.

Tapia L, Kuryatov A, Lindstrom J (2007) Ca2+ Permeability of the (a4)3(b2)2 Stoichiometry Greatly Exceeds That of (a4)2(b2)3 Human Acetylcholine Receptors. Molecular Pharmacology 71:769–776.

Tennant KA, Jones TA (2009) Sensorimotor behavioral effects of endothelin-1 induced small cortical infarcts in C57BL/6 mice. Journal of Neuroscience Methods 181:18–26.

Terry AV, Hernandez CM, Buccafusco JJ, Gattu M (2000) Deficits in spatial learning and nicotinic-acetylcholine receptors in older, spontaneously hypertensive rats. Neuroscience 101:357–368.

Thompson SA, Smith O, Linn DM, Linn CL (2006) Acetylcholine neuroprotection against glutamate-induced excitotoxicity in adult pig retinal ganglion cells is partially mediated through alpha4 nAChRs. Experimental Eye Research 83:1135–1145.

Uchida S, Hotta H, Kawashima K (2009) Long-term nicotine treatment reduces cerebral cortical vasodilation mediated by alpha4beta2-like nicotinic acetylcholine receptors in rats. European Journal of Pharmacology 609:100–104.

Uchida S, Kagitani F, Nakayama H, Sato A (1997) Effect of stimulation of nicotinic cholinergic receptors on cortical cerebral blood flow and changes in the effect during aging in anesthetized rats. Neuroscience Letters 228:203–206.

Unwin N (1993) Nicotinic acetylcholine receptor at 9A resolution. Journal of Molecular Biology 229:1101–1124.

Unwin N (1998) The nicotinic acetylcholine receptor of the Torpedo electric ray. Journal of Structural Biology 121:181–190.

Unwin N (2005) Refined structure of the nicotinic acetylcholine receptor at 4A resolution. Journal of Molecular Biology 346:967–989.

Wada E, Wada K, Boulter J, Deneris E, Heinemann S, Patrick J, Swanson LW (1989) Distribution of alpha2, alpha3, alpha4, and beta2 neuronal nicotinic receptor subunit mRNAs in the central nervous system: A hybridization histochemical study in the rat. Journal of Comparative Neurology 284:314–335.

Wang L, Kittaka M, Sun N, Schreiber SS, Zlokovic B V (1997) Chronic nicotine treatment enhances focal ischemic brain injury and depletes free pool of brain microvascular tissue plasminogen activator in rats. Journal of Cerebral Blood Flow and Metabolism 17:136–146.

Watson BD, Dietrich WD, Busto R, Wachtel MS, Ginsberg MD (1985) Induction of reproducible brain infarction by photochemically initiated thrombosis. Annals of Neurology 17:497–504.

Welsh FA, O'Connor MJ, Marcy VR, Spatacco AJ, Johns RL (1982) Factors limiting regeneration of ATP following temporary ischemia in cat brain. Stroke 13:234–242.

Wetscher GJ, Bagchi D, Perdikis G, Bagchi M, Redmond EJ, Hinder PR, Glaser K, Hinder R a (1995a) In vitro free radical production in rat esophageal mucosa induced by nicotine. Digestive Diseases and Sciences 40:853–858.

Wetscher GJ, Bagchi M, Bagchi D, Perdikis G, Hinder PR, Glaser K, Hinder RA (1995b) Free Radical Production in Nicotine Treated Pancreatic Tissue. Free Radical Biology & Medicine 18:877–882.

Whiting P, Lindstrom J (1986a) Purification and characterization of a nicotinic acetylcholine receptor from chick brain. Biochemistry 25:2082–2093.

Whiting P, Lindstrom J (1986b) Pharmacological Receptors Properties of Immuno-Isolated Neuronal Nicotinic Receptors. Journal of Neuroscience 6:3061–3069.

Witte OW, Bidmon HJ, Schiene K, Redecker C, Hagemann G (2000) Functional differentiation of multiple perilesional zones after focal cerebral ischemia. Journal of Cerebral Blood Flow and Metabolism 20:1149–1165.

Wonnacott S (1997) Presynaptic nicotinic ACh receptors. Trends in Neurosciences 20:92–98.

Xiao C, Nashmi R, McKinney S, Cai H, McIntosh JM, Lester HA (2009a) Chronic nicotine selectively enhances alpha4beta2* nicotinic acetylcholine receptors in the nigrostriatal dopamine pathway. Journal of Neuroscience 29:12428–12439.

Xiao C, Yang K, Zhou C, Jin G, Wu J, Ye J (2009b) Nicotine modulates GABAergic transmission to dopaminergic neurons in substantia nigra pars compacta. Acta Pharmacologica Sinica 30:851–858.

Yaguchi T, Nishizaki T (2010) Extracellular high K+ stimulates vesicular glutamate release from astrocytes by activating voltage-dependent calcium channels. Journal of Cellular Physiology 225:512–518.

Ye Z-C, Sontheimer H (1996) Cytokine modulation of glial glutamate uptake: A possible involvement of nitric oxide. Neuroreport 7:2181–2185.

Zhang Y, Xu Z, Wang H, Dong Y, Shi HN, Culley DJ, Crosby G, Marcantonio ER, Tanzi RE, Xie Z (2012) Anesthetics isoflurane and desflurane differently affect mitochondrial function, learning, and memory. Annals of Neurology 71:687–698.

Zhang ZW, Vijayaraghavan S, Berg DK (1994) Neuronal acetylcholine receptors that bind alpha-bungarotoxin with high affinity function as ligand-gated ion channels. Neuron 12:167–177.

Zidovetzki R, Chen P, Fisher M, Hofman FM, Faraci FM (1999) Nicotine Increases Plasminogen Activator Inhibitor-1 Production by Human Brain Endothelial Cells via Protein Kinase C Associated Pathway. Stroke 30:651–655.

Zouridakis M, Zisimopoulou P, Poulas K, Tzartos SJ (2009) Recent advances in understanding the structure of nicotinic acetylcholine receptors. IUBMB Life 61:407–423.